

T-2195

APPLICATIONS OF A NaI(Tl) SCINTILLATOR
AS A FAST NEUTRON DETECTOR TO
DFN URANIUM EXPLORATION

by

Martin Rymes

ProQuest Number: 11016566

All rights reserved

INFORMATION TO ALL USERS

The quality of this reproduction is dependent upon the quality of the copy submitted.

In the unlikely event that the author did not send a complete manuscript and there are missing pages, these will be noted. Also, if material had to be removed, a note will indicate the deletion.



ProQuest 11016566

Published by ProQuest LLC (2019). Copyright of the Dissertation is held by the Author.

All rights reserved.

This work is protected against unauthorized copying under Title 17, United States Code
Microform Edition © ProQuest LLC.

ProQuest LLC.
789 East Eisenhower Parkway
P.O. Box 1346
Ann Arbor, MI 48106 – 1346

A thesis submitted to the Faculty and the Board of Trustees of the Colorado School of Mines in partial fulfillment of the requirements for the degree of Master of Science (Physics).

Golden, Colorado

Date 4/27, 19 79

Signed:

Martin D. Rymes
Martin D. Rymes
Student

Approved:

F. E. Cecil
F. E. Cecil
Thesis Advisor

Golden, Colorado

Date 4/26, 19 79

F. D. Schowengerdt
F. D. Schowengerdt
Head of Department

ABSTRACT

"I have investigated the use of a NaI(Tl) detector as a fast neutron monitor in delayed fission neutron (DFN) Uranium exploration. I have found that the NaI(Tl) detector may not be used as the detector of the Uranium delayed fission neutrons because a 2.8 MeV neutron source produces the reaction $^{127}\text{I}(n,\gamma)^{128}\text{I}$, which obscures the 57-KeV DFN spectral peak. A 14.1 MeV neutron source further obscures the peak through the reaction $^{23}\text{Na}(n,p)^{23}\text{Ne}$. The NaI(Tl) detector may be used as an effective real time source monitor because it is insensitive to environmental changes and linear in response to a total count rate of approximately 600 counts/second. Because of the production of thermal electrons in the photomultiplier tube, the detector is inoperative at temperatures greater than 120°C.

TABLE OF CONTENTS

	<u>Page</u>
LIST OF TABLES	vii
LIST OF FIGURES	viii
INTRODUCTION	1
PART I	
PURPOSE	5
INTRODUCTION	5
OPTIMUM DETECTOR GAMMA SHIELDING	
Introduction	8
Procedure	8
Conclusion	9
DETECTION OF DELAYED FISSION NEUTRONS INDUCED BY A MONOENERGETIC 2.8 MeV NEUTRON SOURCE	
Introduction	11
Procedure	11
Analysis	13
DETECTION OF DELAYED FISSION NEUTRONS INDUCED BY A MONOENERGETIC 14.1 MeV NEUTRON SOURCE	
Introduction	15
Procedure	15
Analysis	16

	<u>Page</u>
VARIATION ON 14.1 MeV EXPERIMENT USING URANIUM SHUTTLE	
Introduction	18
Procedure	18
Analysis	19
CONCLUSION TO PART I	20
PART II	
INTRODUCTION	21
EFFECT OF CHANGE OF SURROUNDINGS	
Purpose	25
Experimental Setup	25
Execution and Analysis	25
Conclusions	26
EFFECT OF TEMPERATURE INCREASE	
Purpose	27
Experimental Setup	27
Execution and Analysis	27
Conclusions	28
DETECTOR RESPONSE TO HIGH NEUTRON FLUX	
Purpose	29
Experimental Setup	29
Execution and Analysis	29
Conclusions	30

	<u>Page</u>
CONCLUSION TO PART II	31
TABLES	32
FIGURES	35
APPENDIX A	
COMPUTER CURVEFITTING BY LEAST-SQUARES METHOD	57
APPENDIX B	
FOUR-STAGE AUTOMATIC SEQUENCING BOX	60
APPENDIX C	
METHOD OF APPROXIMATING DFN YIELD	63
REFERENCES	65

LIST OF TABLES

<u>Table</u>		<u>Page</u>
I	THICKNESS OF STEEL GAMMA SHIELDING VS. AREA UNDER PEAK	32
II	57 KeV PEAK AREA AS A FUNCTION OF TEMPERATURE	33
III	DETECTOR RESPONSE TO NEUTRON SOURCE VS. PROXIMITY (CENTER OF DETECTOR TO SOURCE)	34

LIST OF FIGURES

<u>Figure</u>		<u>Page</u>
1	CROSS SECTION FOR THE PRODUCTION OF THE FIRST EXCITED STATE IN ^{127}I	35
2	EXPERIMENTAL SETUP FOR DETER- MINING OPTIMUM GAMMA SHIELDING	36
3	SAMPLE DATA OBTAINED FROM OPTIMUM SHIELDING EXPERIMENT	37
4	AREA OF PEAK REGION (INCLUDING BACKGROUND) VS. THICKNESS OF STEEL SHIELDING	38
5	THE LEAD PIG	39
6	CALIBRATION SPECTRUM OF 2 Ci PuBe SOURCE FOR 2.8 MeV DFN EXPERIMENT	40
7	EXPERIMENTAL SETUP FOR CALIBRATING THE 2.8 MeV NEUTRON SOURCE	41
8	EXPERIMENTAL SETUP FOR DETECTING DELAYED FISSION NEUTRONS PRODUCED BY A 2.8 MeV NEUTRON SOURCE	42
9	ENERGY SPECTRUM OF 2.8 MeV NEUTRON ACTIVATION EXPERIMENT	43
10	MULTISCALE OF PEAK REGION FOLLOWING 2.8 MeV NEUTRON ACTIVATION EXPERIMENT	44
11	EXPERIMENTAL SETUP FOR DETECTING DELAYED FISSION NEUTRONS PRODUCED BY A 14.1 MeV NEUTRON SOURCE	45
12	ENERGY SPECTRUM OF 14.1 MeV NEUTRON ACTIVATION EXPERIMENT	46
13	LOGARITHMIC MULTISCALE PLOT OF PEAK REGION FOLLOWING 14.1 MeV NEUTRON ACTIVATION EXPERIMENT	47

<u>Figure</u>		<u>Page</u>
14	EXPERIMENTAL SETUP FOR 14.1 MeV BOMBARDMENT USING URANIUM SHUTTLE	48
15	ENERGY SPECTRUM OF 14.1 MeV URANIUM SHUTTLE EXPERIMENT	49
16	MULTISCALE OF PEAK REGION FOLLOWING 14.1 MeV URANIUM SHUTTLE EXPERIMENT	50
17	EXPERIMENTAL SETUP TO DETER- MINE ENVIRONMENTAL DEPENDENCE	51
18	EXPERIMENTAL SETUP TO DETER- MINE TEMPERATURE DEPENDENCE	52
19	ENERGY SPECTRA ILLUSTRATING THERMO- ELECTRIC ENCROACHMENT UPON 57 KeV PEAK	53
20	EXPERIMENTAL SETUP TO DETERMINE DETECTOR RESPONSE TO HIGH NEUTRON FLUX	54
21	PULSE SHAPE OF DIFFERENTIALLY AMPLIFIED PHOTOMULTIPLIER TUBE OUTPUT	55
22	DETECTOR COUNT RATE VS. $1/r^2$, 5-MINUTE SAMPLES; A PLOT OF TABLE III	56

ACKNOWLEDGEMENTS

I would like to thank the U. S. Geologic Survey for which this work was done under USGS Grant #14-08-0001-G-548. I must also thank Dr. F. E. Cecil for his guidance, J. P. Kintner for his advice and assistance in fabricating equipment, and Geroge Leon for sharing his electronics expertise. To my parents, Ivan and June Rymes, who affirmed me, I must also express my gratitude.

INTRODUCTION

The method of Uranium assay logging that employs a pulsed neutron source and detection of delayed fission neutrons requires a sensitive detector of delayed fission neutrons and an accurate neutron flux monitor. The technique employs the fact that, following bombardment of Uranium bearing ore by neutrons, a small percent of the fission products of Uranium release neutrons in their decay schemes. Because there are several different fission products that release delayed fission neutrons, each with a different half-life, the half-life of the delayed fission neutrons cannot be well-defined. However, data on relative abundances and half-lives of delay chains are available (1), from which the time dependence of delayed fission neutrons can be calculated. As delayed neutrons constitute only 2 to 3% of the total number of fission neutrons (2), the neutron spectrum cannot be measured during the Uranium bombardment, because this low flux is caused by a high flux of source neutrons which, if detected, would obscure the data of interest. To circumvent this problem, the neutron source is pulsed and the neutron spectrum is sampled cyclically between neutron bombardment and sampling on

the order of the recovery time of the detector. Such practical considerations as detector response time and attenuation of neutron flux during source shutoff raise the practical waiting time. The length of time of the neutron bombardment is based upon the total desired neutron output, and the time required for the detector to sample the delayed fission neutrons should span several optimum half-lives (from a few seconds to a few minutes). The neutron source can be pulsed as soon after sampling as is desirable. The total cycling scheme, therefore, can be divided into four stages:

1. Neutron source on--until rate of delayed fission neutrons is saturated.
2. Waiting time--from a few milliseconds to a few seconds.
3. Detector spectrum sampled--a few seconds to a few minutes.
4. Null time--as short as desired.

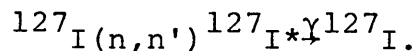
Since the NaI(Tl) scintillation detector can be a high-efficiency fast neutron detector (3,4,5), it may serve to detect both the delayed fission neutrons and the source neutrons, solving the problems both of Uranium assaying through detection of delayed fission neutrons

and of accurate source monitoring. The last function cannot be neglected, for it is clear that if geometry and efficiency factors remain constant, the amount of delayed fission neutrons detected is directly proportional to the amount of Uranium in the sampling region and to the neutron flux through the sample, itself linearly dependent upon the source intensity. Re-expressed,

$$U=kD/I,$$

U being the Uranium concentration, D being the detected number of delayed fission neutrons, I being neutron source intensity, and k being a constant of proportionality. In general, the source monitoring problem applies to all forms of neutron activation analysis, and therefore has a broader application.

The method of neutron detection employed by the NaI(Tl) scintillation detector utilizes the self-detection of the 57-KeV gamma ray emitted by the prompt de-excitation of the Iodine in the crystal that undergoes the reaction



The cross-sections for this reaction have been measured for various incident neutron energies (6,7), and the results are in Figure 1. The unique feature of the NaI(Tl) detector is that it is not activated unless

neutrons of energy exceeding 57 KeV are incident upon it. Since its response is flat to within 40% in the neutron energy range of interest (0.5-14.1 MeV), it provides a relatively unbiased instantaneous fast neutron flux monitor. As it does not respond to thermal neutron flux, it is less sensitive to the characteristics of its surroundings, which frequently thermalize neutrons, than other source monitor detectors. Other direct neutron detection schemes, e.g., those employing the reaction $^{10}\text{B}(n,\alpha)^7\text{Li}$ or $^3\text{He}(n,p)\text{T}$ (8,9), have high thermal neutron cross-sections, and are used inferentially by means of assumptions about the surrounding medium.

The problem of Uranium assay logging by detection of delayed fission neutrons utilizing a NaI(Tl) detector, then, is two-fold and will be treated as two separate problems here. Part 1 explores the feasibility of employing a NaI(Tl) detector as a detector of delayed fission neutrons from Uranium, and Part 2 investigates the feasibility of using a NaI(Tl) scintillator as neutron source monitor.

PART I

PURPOSE

Part 1 investigates the feasibility of employing a NaI(Tl) scintillator detector as a detector of Uranium delayed fission neutrons.

INTRODUCTION

As was outlined above, the method of detection of delayed fission neutrons investigated involves alternately pulsing a neutron source and turning on a multichannel analyzer attached to a NaI(Tl) scintillator in order to observe the 57 KeV ^{127}I de-excitation gamma ray that indicates incident fast neutron flux from the bombarded Uranium. Since 57 KeV is lower energy than most of the gamma rays emitted by the daughters in the Uranium decay chain and since a high flux of gamma rays of energy greater than 57 KeV would produce a high Compton background that would interfere with the neutron-induced 57-KeV peak, the detector must be shielded against gamma rays, while still permitting penetration of fast neutrons. Lead is the obvious choice of shielding material, but it has the drawback of the 88 KeV Pb K shell x-ray which is produced by the passage of any primary or secondary

ionizing radiation through the lead. The shielding selected is steel, which is nearly as effective a gamma shield as lead without the drawback, since the Fe K x-ray is 6 KeV.

Although the conventional pulsed neutron sources are 14 MeV monoenergetic neutron sources, a 3 MeV source is used initially, because it is below the energy threshold for production of delayed fission neutrons by $^{17}\text{O}(n,p)^{17}\text{N} \rightarrow ^{17}\text{O} + n + ^{16}\text{O}$, $Q = -7.93$ MeV (10). This interfering reaction provides the ultimate limit to the sensitivity of the delayed fission neutron Uranium probe (11). Its drawback is lower flux and penetration, but if detection is feasible, guesswork about the Oxygen content of the surrounding medium will be eliminated.

Since 14 MeV neutron sources are conventionally used, and since a 14 MeV source provides a higher flux of neutrons than a 3 MeV source, we also conducted experiments simulating borehole conditions with a 14 MeV neutron source; one in which the detector was a few centimeters from the source, and the other in which the detector was over a meter from the source.

In order to avoid analyzing the neutron flux while the neutron source is on, a waiting period of

5 seconds was selected. Both bombardment and analysis times were arbitrarily established at 10 seconds, and the null time was set at 5 seconds to clearly avoid turning on the source while the analyzer was recording.

OPTIMUM DETECTOR GAMMA SHIELDING

Introduction

This experiment establishes the optimum thickness of steel that would freely permit fast neutrons to enter the NaI(Tl) scintillation detector with maximum shielding from gamma rays from low grade Uranium ore, as explained in the introduction to Part 1. When this is known, a shield using the optimum design can be constructed that would improve statistics by reducing the background without changing the peak characteristics significantly.

Procedure

The experiment was set up as in Figure 2. A 2 Ci PuBe source, emitting 3×10^6 n/s (12), was enclosed by 3" of lead to stop its emitted gamma rays. The detector was placed in a 1/4" steel pipe surrounded by 2" of lead and recessed 2" to greatly reduce the background and scattering from the surroundings. The detector was situated 1 meter from the source corresponding to neutron flux at the detector of approximately $10 \text{ n cm}^{-2} \text{ s}^{-1}$. The face of the detector towards the source was unshielded. The Uranium placed between the source and the detector was a paper bag containing 960 g of .44 w/o Uranium ore obtained

from the Colorado School of Mines Research Institute. Different thicknesses of steel (9/16", 1/2", 3/8", 1/4", 1/8", 0") were placed between the ore and the detector, and the energy spectrum was sampled for 300 seconds for each shielding thickness.

Analysis

The data obtained from the multichannel analyzer were interpreted by computer curvefitting (see Appendix A). Two samples of the raw data are given in Figure 3. Table 1 lists the peak area for each thickness. Figure 4 is a plot of the background level for each thickness. Figure 3 demonstrates the ease at which a rough qualitative analysis can be made, since the peak is clearly visible in Figure 3a and engulfed by the background in Figure 3b. Table 1 suggests a breakdown in information usefulness between 3/8" and 1/4", substantiated by the noise-level plot in Figure 4.

Conclusion

If steel is the only shielding material between Uranium ore and a NaI(Tl) scintillation detector, a minimum thickness of 3/8" is required if a neutron flux of $10 \text{ n cm}^{-2} \text{ s}^{-1}$ is to be measured in a relatively short period of time (one or two minutes). Since more steel

adds to bulk and mass without significantly reducing background noise, 3/8" is the optimum thickness of steel shielding, with negligible effect on fast neutrons.

DETECTION OF DELAYED FISSION NEUTRONS INDUCED
BY A MONOENERGETIC 2.8 MEV NEUTRON SOURCE

Introduction

The Introduction to Part 1 laid out the method of detecting delayed fission neutrons from Uranium ore. In this experiment, the neutron source was a monoenergetic neutron flux produced by accelerating deuterons into a deuterium-doped target, yielding the reaction $d + d \rightarrow {}^3\text{He} + n$, the neutron having an energy of 2.8 MeV (13). A 150 KeV Nuclear Data neutron generator with a deuterated titanium target provided the source of 2.8 MeV monoenergetic neutrons.

Procedure

The neutron flux from the accelerator was inferred by using the known 3×10^6 n/s intensity of the 2 Ci PuBe source. This source was placed 1 meter away from the detector, the detector being placed in a pig. This pig is composed of lead surrounding a 1/4" steel pipe as illustrated in Figure 5. A 5-minute count was taken, and the spectrum (Figure 6) was analyzed by computer (see Appendix A) to yield a 57 KeV peak of 6317 ± 154 counts.

The detector was placed at a distance of 3 meters from the 2.8 MeV monoenergetic neutron flux emitted from the target of the accelerator, as in Figure 7. The accelerator high voltage was 150 KeV and the beam current was 200 μ A.

Since the flux of an isotropic neutron source is linearly proportional to the intensity and inversely proportional to the square of the distance from the detector to the source, the neutron intensity from the accelerator can be easily calculated. The measured 57 KeV peak of a 30-second bombardment from accelerator neutrons was 6254 ± 220 counts. Since the bombardment time was 10% of the PuBe bombardment time, the total number of counts must be multiplied by 10, and the intensity produced by the accelerator at 200 μ A beam current and 150 KV high voltage was 2.7×10^8 n/s. This method of measuring the output of the neutron source agreed with the output inferred using the previously measured values of the $^{127}\text{I}(n,n')^{127}\text{I}^*$ cross section (3).

The pig was then placed 3 cm from the accelerator as shown in Figure 8, and the following manually-controlled sequence was employed:

BEAM ON	10 seconds
OFF	5 seconds
ANALYZER ON	10 seconds
OFF	5 seconds

The Uranium used was 20 g of pure U_3O_8 in a plastic bag taped to the face of the pig.

Sixty sequencing cycles were completed. The results are plotted in Figure 9. As can be seen, no peak at 57 KeV is evident due to the high background. In an effort to understand this background, the number of counts in the region in which the peak was expected was multi-scaled at a dwell time of 2 minutes for several hours following the bombardment. This multiscale is shown in Figure 10, after the 1800-count room background was subtracted.

Analysis

The calculation done in Appendix C for the expected number of delayed fission neutrons is based upon the detector efficiency and geometry factors. A spherical geometry can be assumed, treating the Uranium as an isotropic point source 5 cm from the detector face, which is 3 cm in radius. The geometric efficiency of the detector relative to the Uranium is, therefore,

$\pi r^2/4\pi R^2 = (r/2R)^2 = 9\%$. The neutron efficiency of the detector is the number of Iodine nuclei in the detector multiplied by the reaction cross-section. For 0.5 MeV neutrons this yields an efficiency, given the thickness of the crystal as 6 cm, of 3% and the total efficiency is then .27%.

The equation in Appendix C, using a distance from accelerator target to Uranium sample of 3 cm, yields a total detected count of delayed fission neutrons of 1500. Since the total peak area is 22,000 counts, this is 7% of the total. However, as this peak is on the side of a broader higher-energy peak (see Figure 9), it is unrecognizable.

The reason for the large background is the thermal neutron capture by ^{127}I , yielding the decay $^{128}\text{I} \rightarrow ^{128}\text{Xe}$, having an energy of 2.125 MeV. This was seen by analyzing the high-energy spectrum and noticing that the broad Compton edge terminates at 2.12 MeV, and by finding that the half-life of the exponential decay plotted in Figure 10 is 25 minutes, the half-life of $^{128}\text{I} \rightarrow ^{128}\text{Xe}$.

DETECTION OF DELAYED FISSION NEUTRONS INDUCED
BY A MONOENERGETIC 14.1 MEV NEUTRON SOURCE

Introduction

Since the Compton edge of the reaction $^{128}_{\text{I}} \beta \rightarrow ^{128}_{\text{Xe}}$ prevented detection of delayed fission neutrons under optimum conditions by the bombardment of 2.8 MeV neutrons, it is expected that this reaction will also inhibit detection of the delayed fission neutrons by a 14.1 MeV source. The 14.1 MeV monoenergetic neutron flux was produced by accelerating deuterons into a tritiated target, producing the reaction $d + t = ^4\text{He} + n$, the neutron's energy being 14.1 MeV (14).

A 90-KV Kaman Sciences neutron generator with a tritiated titanium target provided the source of 14.1 MeV monoenergetic neutrons.

Procedure

The detector in the pig was placed directly in front of the accelerator with 20 g of U_3O_8 in a plastic bag placed in an aluminum shuttle between the detector and the accelerator, as in Figure 11. The bombardment and spectrum sampling were governed by a four-stage automatic pulsing box (Appendix B) adjusted to the following times:

BEAM ON	10 seconds
OFF	6 seconds
ANALYZER ON	10 seconds
OFF	6 seconds

The accelerator high voltage was 90 KV and the beam current was 200 μ A. Twenty sequencing cycles were completed, the resulting spectrum plotted in Figure 12. The 57 KeV region was multiscaled at .5 seconds per channel, plotted in Figure 13.

Analysis

There are 15,000 counts in the 101-180 channel peak region. The predicted number of counts due to Uranium delayed fission neutrons can be found by the method of Appendix C. The distance from the target to the Uranium is 4 cm, and the geometric efficiency (by the method on page 13) is 3.5%.

Therefore, the predicted number of counts due to Uranium delayed fission neutrons is 32, or 0.2% of the total. This is clearly negligible. Figure 13 indicates that the exponential decay of the background is a superposition of a short-term 38-second half-life upon a long-term 25-minute half-life. The 25-minute half-life is attributable to the thermal capture of neutrons by ^{127}I ,

leading to the decay $^{128}\text{I} \xrightarrow{\beta^-} ^{128}\text{Xe}$, as in the 2.8 MeV experiment. The 38 second half-life corresponds to the reaction $^{23}\text{Na}(n,p)^{23}\text{Ne} \xrightarrow{\beta^-} ^{23}\text{Na}$, which has an energy threshold of 3.9 MeV (15).

VARIATION ON 14.1 MEV EXPERIMENT
USING URANIUM SHUTTLE

Introduction

The entire procedure in this experiment is identical to the previous one (pp. 15-17), save that an attempt to cut down the background due to the ^{23}Na and ^{127}I neutron reactions was made by placing the detector farther from the source. This also corresponds to realistic downhole logging tools, since the detector and source in a logging tool would be placed far from each other, the source inducing reactions in the surroundings to which the detector responds as it passes the same area shortly thereafter.

To duplicate the effect of a tool passing a Uranium deposit, Uranium was shuttled between the source and detector.

Procedure

Figure 14 illustrates the relative placements of detector, accelerator, and shuttle. This is a low-speed air shuttle, requiring a few seconds for transit, which is acceptable, as the waiting time had previously been measured in seconds. The manual four-stage sequencing was:

BEAM ON	U AT SOURCE	20 seconds
OFF	U TO DETECTOR	5 seconds
ANALYZER ON	U AT DETECTOR	20 seconds
OFF	U TO SOURCE	15 seconds

The only other characteristic that changed from the previous experiment to this one is the distance of the detector from the source, 1.6 meters.

The sequence was cycled 10 times. The results are shown in Figure 15.

The high-energy spectrum was then multiscaled by hand in the manner described on page 13, save that the dwell time was 5 minutes. The results, after removal of a 2200-count natural background, are plotted in Figure 16.

Analysis

The calculation in Appendix C is virtually unchanged from that performed in the last experiment, save that the time spans have changed. The predicted number of delayed fission neutrons detected from the Uranium is, then, 30. Although the background has dropped to 2000 counts, it is obvious that the peak still remains undetectible. The multiscaling plotted in Figure 16 indicates a large contribution from the thermal capture of neutrons by ^{127}I .

CONCLUSION TO PART I

The NaI(Tl) scintillation detector appears to be inappropriate as a detector of Uranium delayed fission neutrons. This is because the neutron capture reaction $^{127}\text{I}(n,\gamma)^{128}\text{I} \xrightarrow{\beta} ^{128}\text{Xe}$, induced when the neutron source is turned on, produces a 2.12 MeV beta particle of half-life 25 minutes. The Compton curve of the beta decay obscures the 57 KeV peak in the NaI(Tl) scintillator, which is the tag of the delayed fission neutrons. For neutron energies above 3.9 MeV, the reaction $^{23}\text{Na}(n,p)^{23}\text{Ne} \xrightarrow{\beta} ^{23}\text{Na}$ also adds a short-lived ($t_{1/2}=38\text{s}$) Compton background, further obscuring the peak.

PART II

INTRODUCTION

As mentioned in the general introduction, the measurement of delayed fission neutrons produced by neutron bombardment of Uranium can be calculated by

$$U = kD/I,$$

U being the Uranium concentration, D being the detected number of delayed fission neutrons, k being a constant of proportionality, and I being the neutron source intensity. It is clear, then, that an accurate measurement of neutron source flux is necessary to correctly interpret any neutron activation data.

Existing source monitoring methods (8,9) are generally dependent upon properties in the surrounding medium to remain constant. One method involves encasing a conventional NaI(Tl) detector in Boron, detecting the 477 KeV gamma ray line from the $^{10}\text{B}(n,\alpha)^7\text{Li}$ reaction. But as this reaction becomes more probable at thermal neutron energies, it means that the detector is more sensitive to thermal neutrons reflected from surrounding media than fast neutrons directly from the source. This dependence upon surroundings is overcome by assuming

that the surrounding media will not vary in neutron reflecting or thermalizing properties significantly, an assumption that is supported by the fact that hitherto there was no better way to monitor the neutron source. This thinking has promoted totally indirect methods of monitoring the source.

One method is based on the assumption that the crust of the Earth has a fairly constant 50% Oxygen content. Then, the neutron source activates the reaction $^{16}\text{O}(n,p)^{16}\text{N}$, which beta decays with a 7 second half-life. The scintillator in this case only detects when the neutron source is off, sampling for a fixed time interval, necessitating integration of the high-energy Compton spectrum and back-extrapolation (16).

Another method is cruder, setting the detector threshold to accept all gammas above the 2.2 MeV deuterium gamma-emission level. The assumption is that the total cross-section for the Earth's crust to react with a neutron and release a gamma ray with energy greater than 2.2 MeV is a constant (16).

The proposed use of the NaI(Tl) scintillation detector as a neutron source monitor is based upon observation of the 57 KeV $^{127}\text{I}(n,n')^{127}\text{I}^*$ de-excitation gamma

ray, as explained in the main introduction. The apparent advantages are that the detector will not respond to a neutron of energy less than 57 KeV, eliminating all but fast neutrons, thus making the detector insensitive to the thermal neutrons reflected by the surroundings; that the detector's fast response allows it to be used as a real time flux monitor, as opposed to the integrating or time-averaged flux monitors; and that the detector is relatively inexpensive. A possible drawback is that production of thermoelectric electrons in the photomultiplier tube would eventually obscure the 57-KeV peak at high temperatures. Of interest is the linearity of response of the detector to increased fast neutron flux, which would establish limits to the source intensity and/or proximity of the detector to the source imposed by pulse pile up.

In the following sections of this report, we will study:

1. the expected insensitivity of the NaI(Tl) detector as a fast neutron monitor to changes in the environment,
2. the temperature dependence of the phototube and critical upper temperature limit,

3. the count rate dependence, to determine the flux at which the count rate deviates from meaning.

EFFECT OF CHANGE OF SURROUNDINGS

Purpose

This experiment investigates the effect of a change in surroundings on the monitoring of neutron flux by a NaI(Tl) scintillation detector.

Experimental Setup

As seen in Figure 17, a hollow steel pipe was placed between the 2 Ci PuBe source and the NaI(Tl) detector to simulate the jacketing of a borehole probe. The lead around the PuBe source shields the detector from the gamma rays emitted by the source, while the 3/8" steel plate in front of the detector shields it from the gamma rays of the surroundings and the 88 KeV neutron-induced Lead x-ray. The first spectrum was taken with free-air surroundings, and concrete blocks were placed on both sides of the steel pipe for the second spectrum.

Execution and Analysis

Two 30-second spectra were taken, the first with free-air surroundings, the second with concrete surroundings. The computer curvefitting (see Appendix A) yielded the following results:

<u>Surroundings</u>	<u>Peak</u>
Free-Air	1459±53
Concrete	1586±54

Conclusions

The difference in peak counts was 127; with standard deviations of 50 counts, there is considerable overlap. The detector response to a highly neutron-reflective medium (concrete) from a neutral environment is therefore quite small. From this, we conclude that the NaI(Tl) scintillation detector as a monitor of fast neutron flux is insensitive to environment.

EFFECT OF TEMPERATURE INCREASE

Purpose

This experiment investigates the effect of thermal black-body electron background buildup on the detection of the 57 KeV peak in the photomultiplier tube abutting the NaI(Tl) scintillation detector and establishes a maximum effective temperature for fast neutron detection.

Experimental Setup

As Figure 18 indicates, the detector was placed in a thermostatically controlled oven with the 2 Ci PuBe source outside the oven 75 cm away from the NaI(Tl) crystal. The PuBe source was surrounded by lead to shield the detector from the emitted gamma rays, and the crystal was surrounded by 3/8"-thick steel to shield from the gamma rays of the surroundings and the 88-KeV neutron-induced Lead x-rays.

Execution and Analysis

Seven 100-second spectra were taken with temperature ranging from 70° F to 270° F. Figure 20 gives the spectra at 200° F, 250° F, and 270° F, in which the thermoelectrons visibly encroach upon the 57 KeV peak.

Computer curvefitting (see Appendix A) yielded the peak data in Table 2.

Conclusions

As is clear from Figure 19, the use of the NaI(Tl) detector as a fast neutron detector is sharply curbed at temperatures greater than 250° F (120° C).

DETECTOR RESPONSE TO HIGH NEUTRON FLUX

Purpose

This experiment establishes the linearity of the NaI(Tl) scintillation detector response to increases in fast neutron flux, thereby establishing a practical limit to neutron flux entering the detector.

Experimental Setup

The detector was placed several distances from the source as indicated in Figure 20. The distances from the center of the detector to the source were 2.56 m, 2.06 m, 1.56 m, 1.06 m, .76 m, .56 m, .36 m, .31 m, .26 m, .21 m, .16 m, and .11 m. The source was a 2 Ci PuBe source, and the detector was shielded from gamma rays by being placed inside the pig. The pulse shape for low count rate is shown in Figure 21.

Execution and Analysis

At each distance of separation of source and detector a 5-minute live-time spectrum was taken, and the results were computer fitted (see Appendix A) and listed in Table 3. A plot of these peak results against the inverse square of the distance appears in Figure 23.

Conclusions

" The practical upper limit for total count rate, as is seen in Figure 22, is approximately 600 counts/second, corresponding to a neutron flux of $1000 \text{ n cm}^{-2} \text{ s}^{-1}$ entering a crystal of diameter 2". It should be noted that this 600 counts/second peak rate corresponds to a total count rate greater than 50,000 counts/second, which is on the order of the saturation level due to a pulse of approximately 5 microsecond duration (see Figure 21). Naturally, such experimental modifications as amplifier integration time, or use of the amplifier with Base Line Restoration will affect the above limit.

CONCLUSION TO PART II

The NaI(Tl) scintillation detector is effective as a neutron source monitor because it is relatively insensitive to changes in environmental media and is instantaneous in response, as opposed to existing flux monitoring methods that are highly sensitive to environmental changes and may require integrating broad-spectrum or time-averaged analysis techniques.

The total count rate of the NaI(Tl) detector must be typically less than 600 counts/second, limiting the distance between the detector and source and the total neutron source output.

The only limitation in borehole applications of the NaI(Tl) detector as a fast neutron source monitor is that the detector becomes inoperative at above 120° C. This corresponds to an average depth of 3 km (17). This depth limitation can be circumvented by cooling the detector.

TABLE I
THICKNESS OF STEEL GAMMA SHIELDING
VS. AREA UNDER PEAK

Thickness (inches)	Area (counts)
0.0	30276
0.125	19321
0.25	15625
0.375	14884
0.5	13924
0.5625	14400

TABLE II
57 KeV PEAK AREA AS A FUNCTION
OF TEMPERATURE

Temperature (°F)	Area (counts)
70	2521± 94
110	1840± 96
160	2130±101
200	2254± 99
225	2202± 99
250	2024±106
270	*****

TABLE III

DETECTOR RESPONSE TO NEUTRON SOURCE VS. PROXIMITY
(CENTER OF DETECTOR TO SOURCE)

Distance (m)	Peak Area (counts)
<u>RUN I</u>	
2.56	2859 \pm 144
2.06	3566 \pm 125
1.56	4525 \pm 133
1.06	8443 \pm 164
0.76	14620 \pm 220
0.56	26785 \pm 271
0.36	57595 \pm 394
0.26	114463 \pm 552
<u>RUN II</u>	
0.36	56141 \pm 387
0.31	74121 \pm 450
0.26	100428 \pm 527
0.21	143708 \pm 659
0.16	226813 \pm 857
0.11	394099 \pm 1295

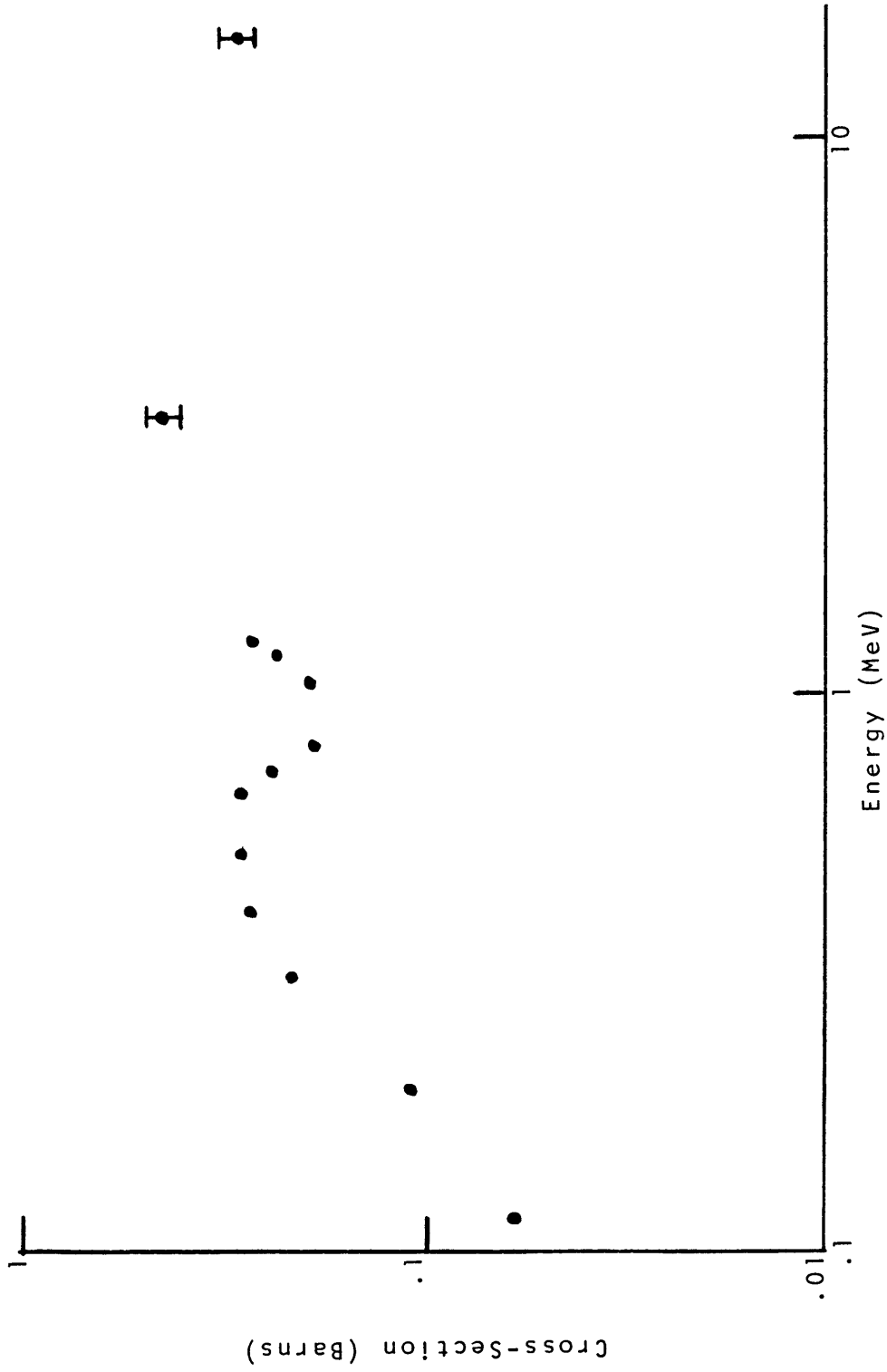


Figure 1: Cross Section for the Production of the First Excited State in ^{127}I (Reference 3)

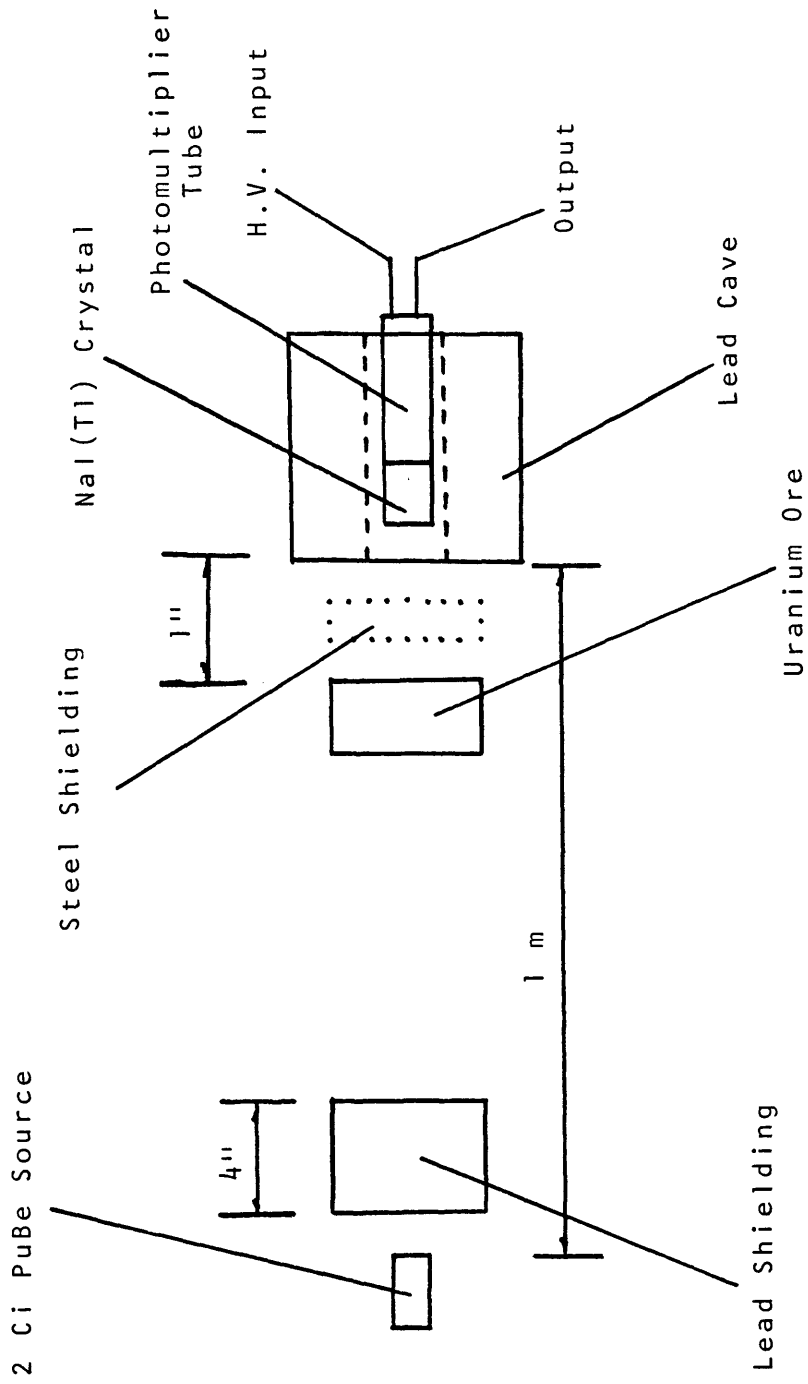


Figure 2: Experimental Setup for Determining Optimum Gamma Shielding

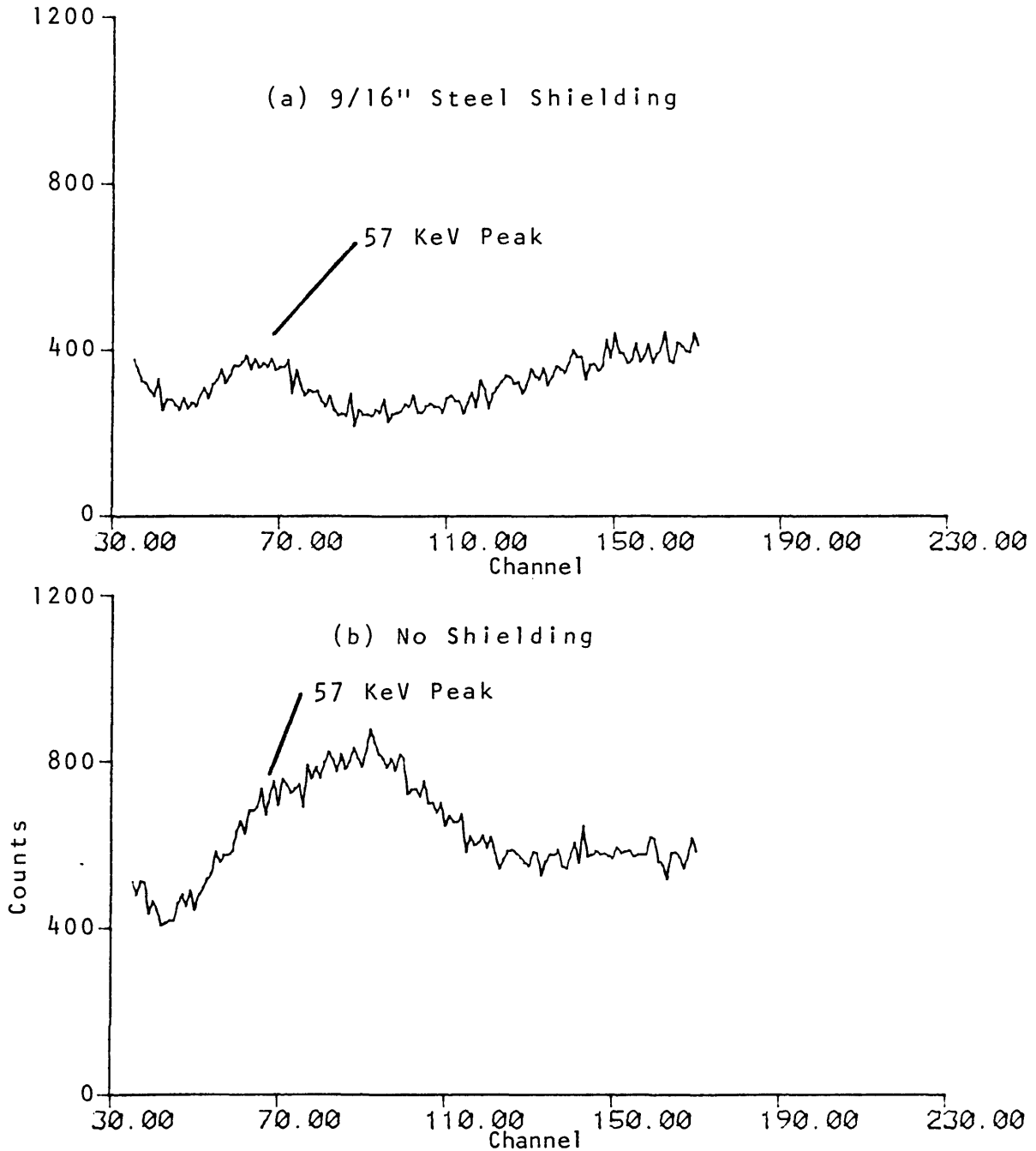


Figure 3: Sample Data Obtained from Optimum Shielding Experiment

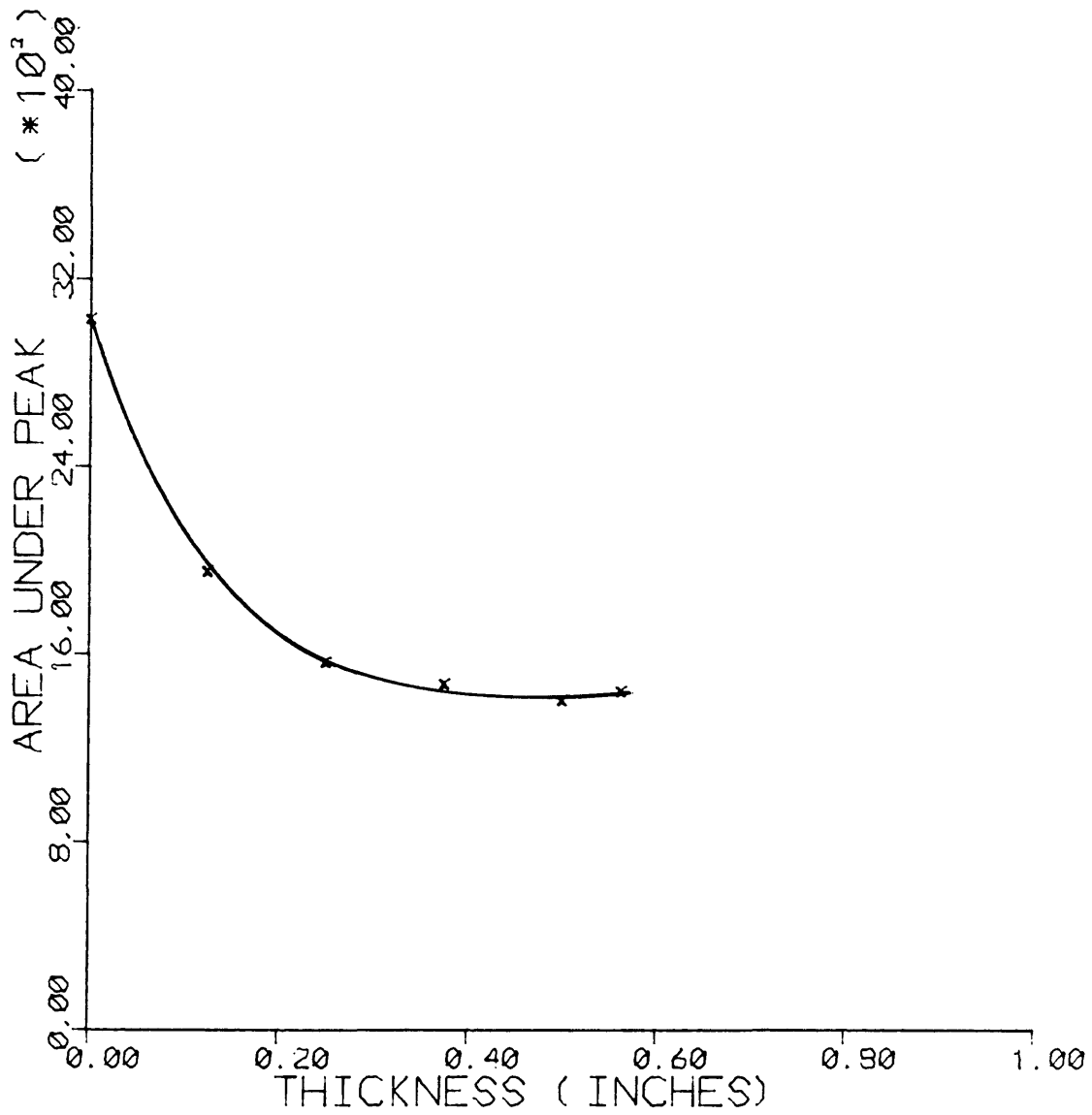


Figure 4: Area of Peak Region (Including Background) vs. Thickness of Steel Shielding

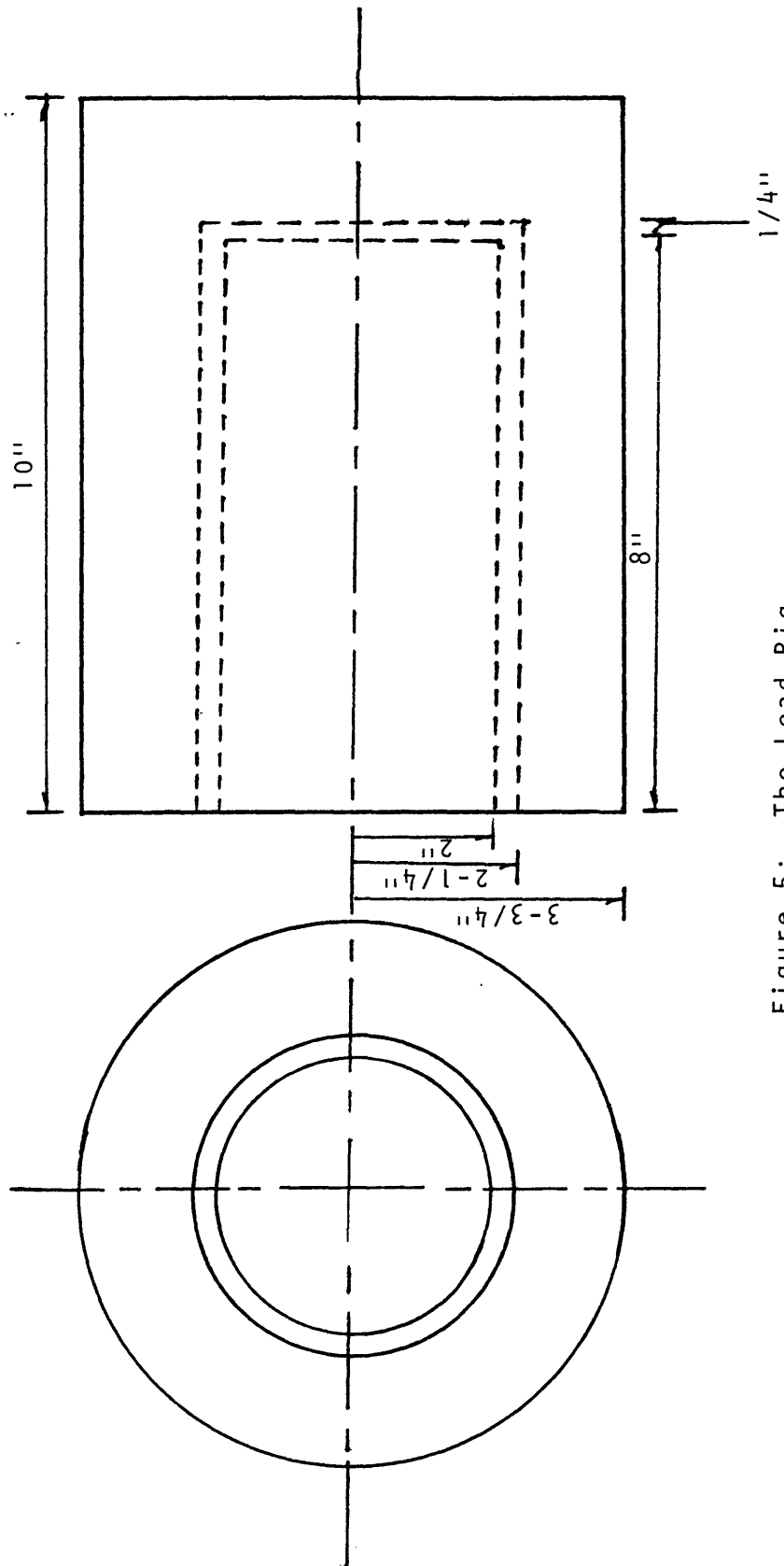


Figure 5: The Lead Pig

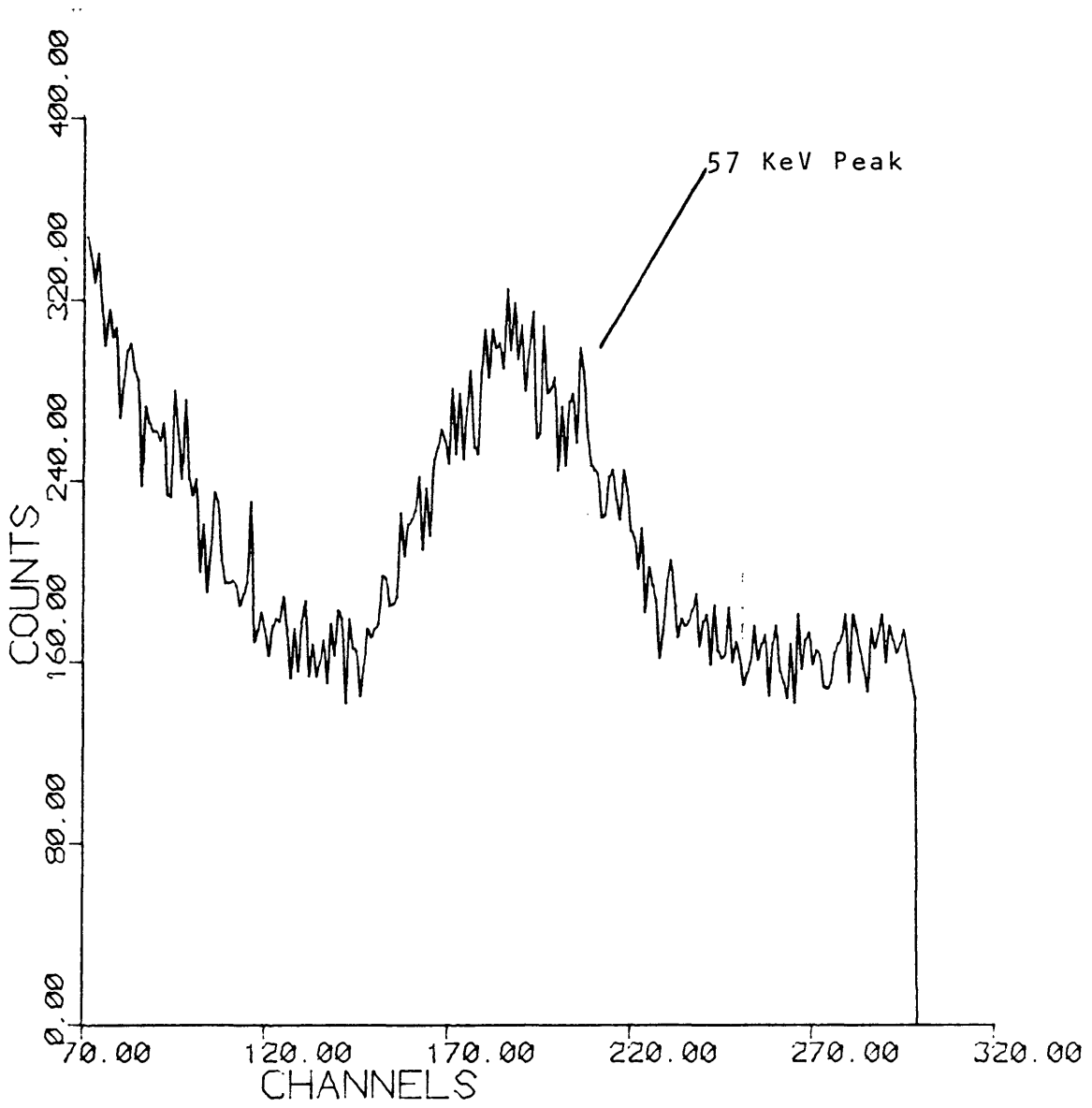


Figure 6: Calibration Spectrum of 2 Ci PuBe Source for 2.8 MeV DFN Experiment

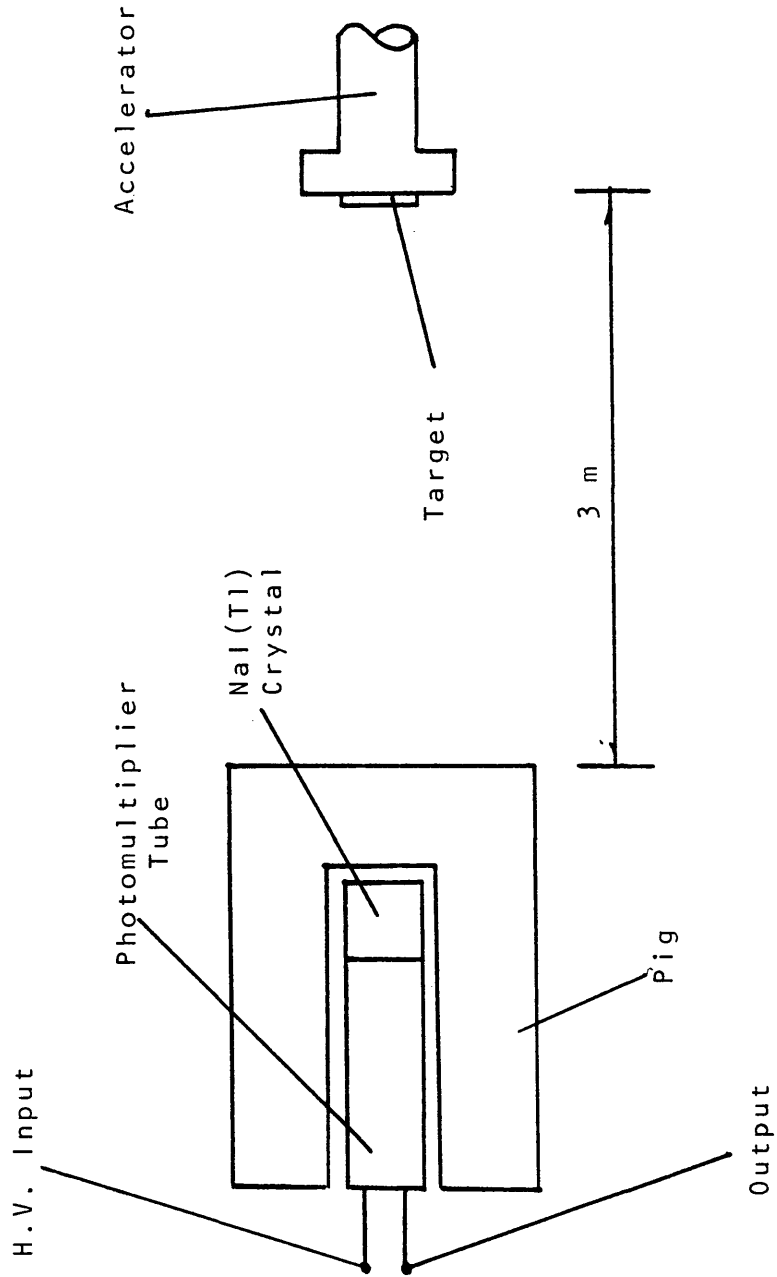


Figure 7: Experimental Setup for Calibrating the 2.8 MeV Neutron Source

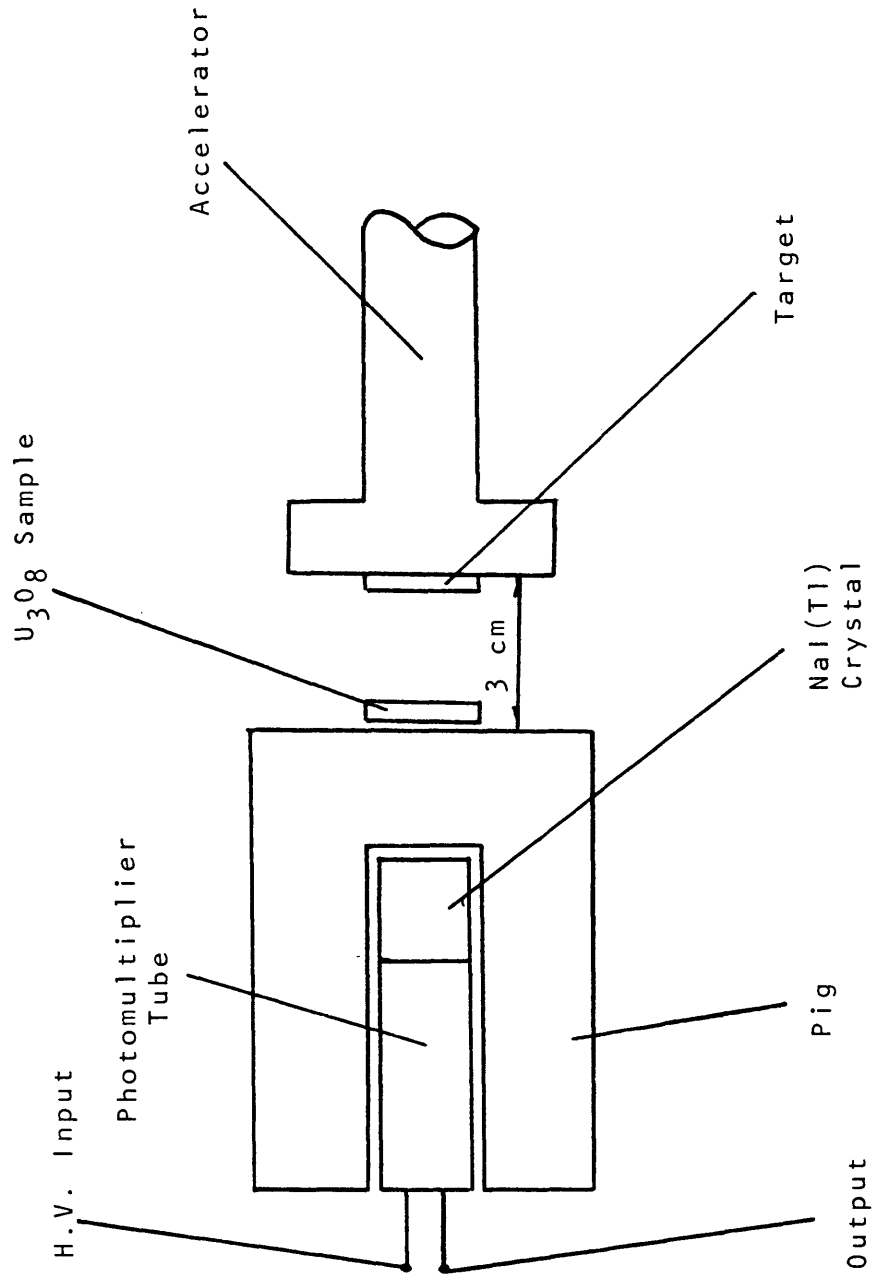


Figure 8: Experimental Setup for Detecting Delayed Fission Neutrons Produced by a 2.8 MeV Neutron Source

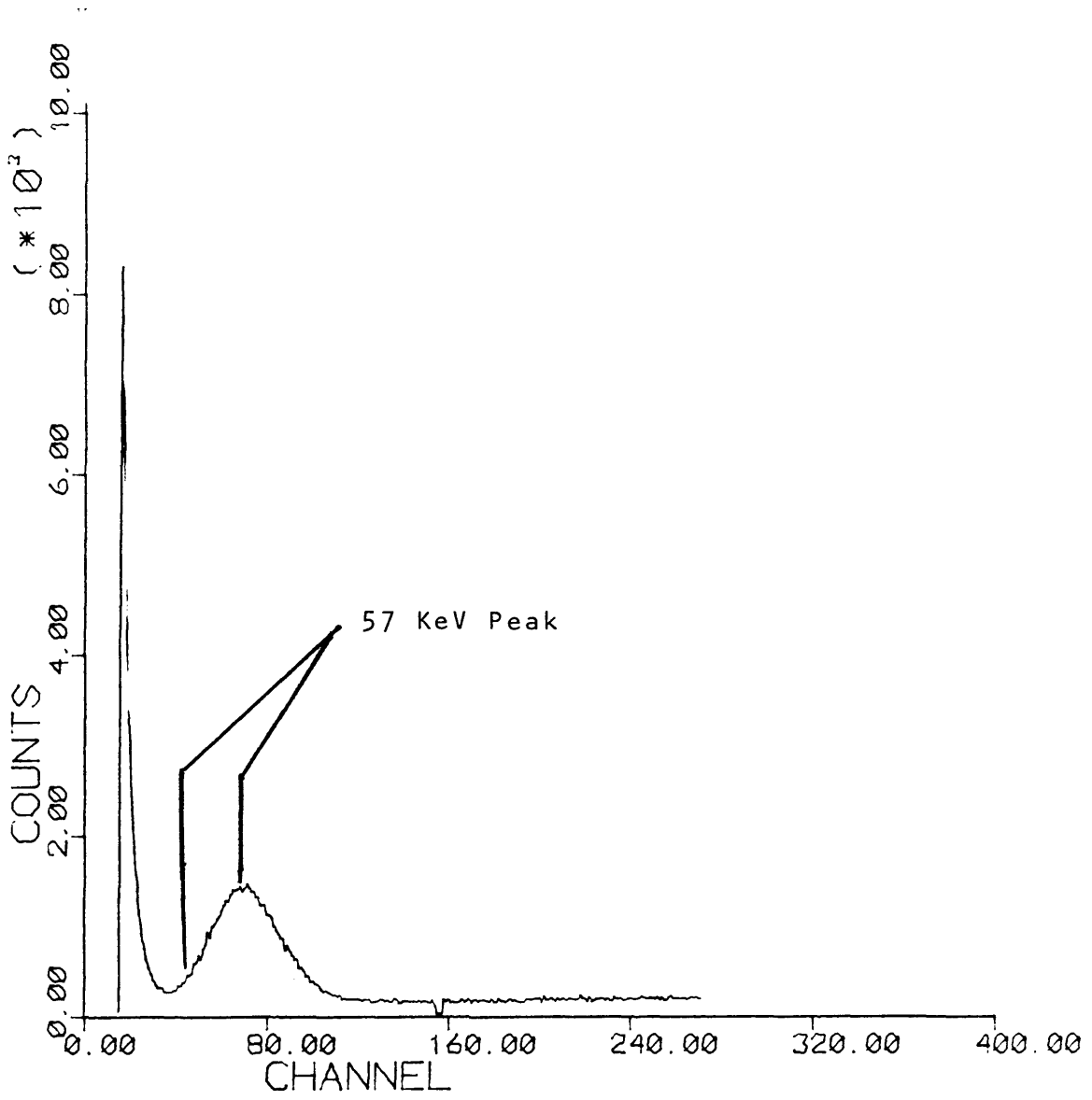


Figure 9: Energy Spectrum of 2.8 MeV Neutron Activation Experiment

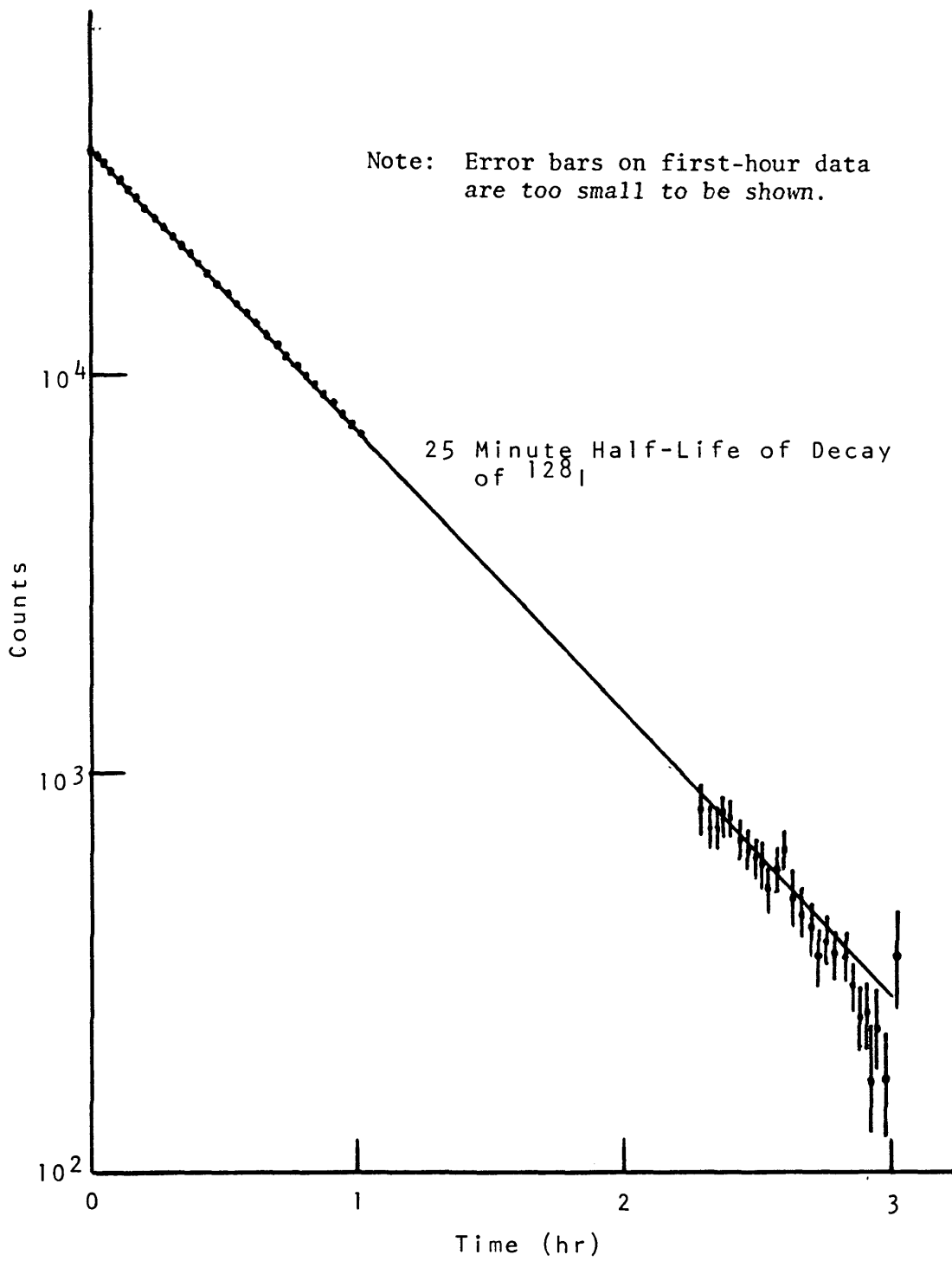


Figure 10: Multiscale of Peak Region Following 2.8 MeV Neutron Activation Experiment

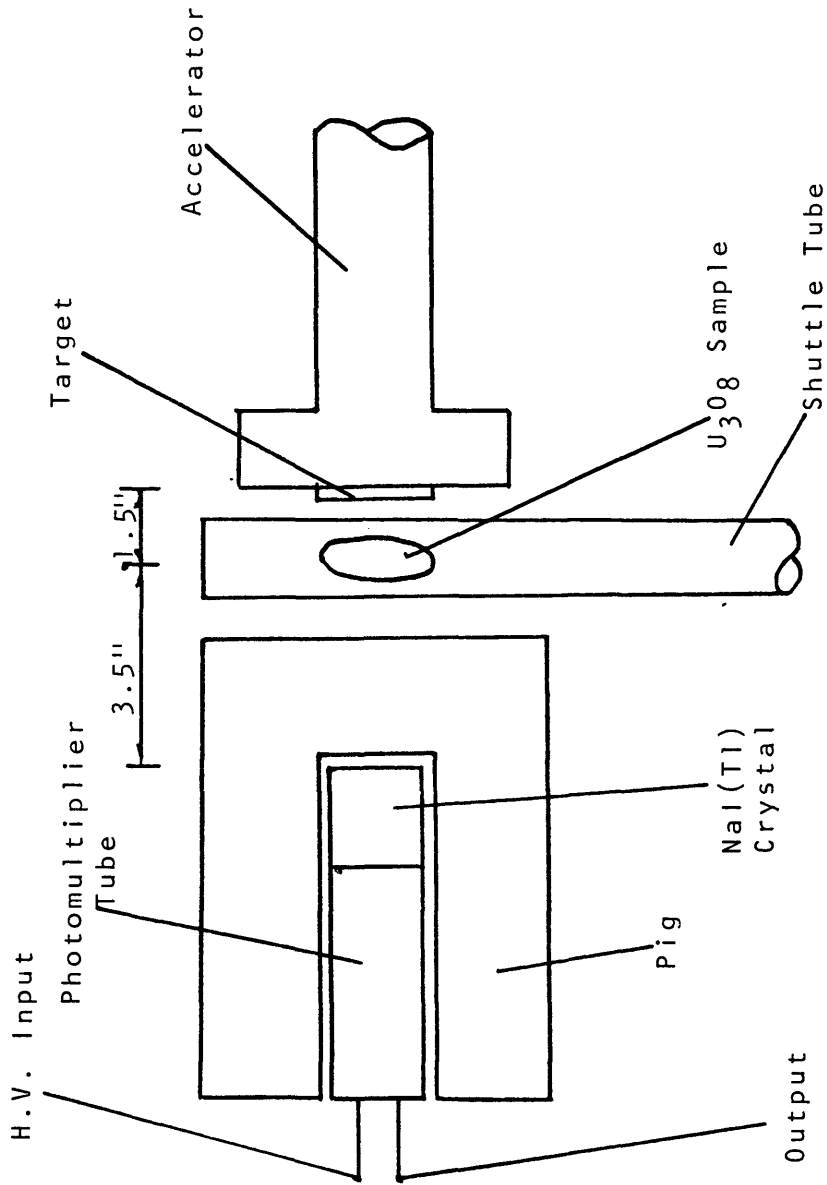


Figure 11: Experimental Setup for Detecting Delayed Fission Neutrons Produced by a 14.1 MeV Neutron Source

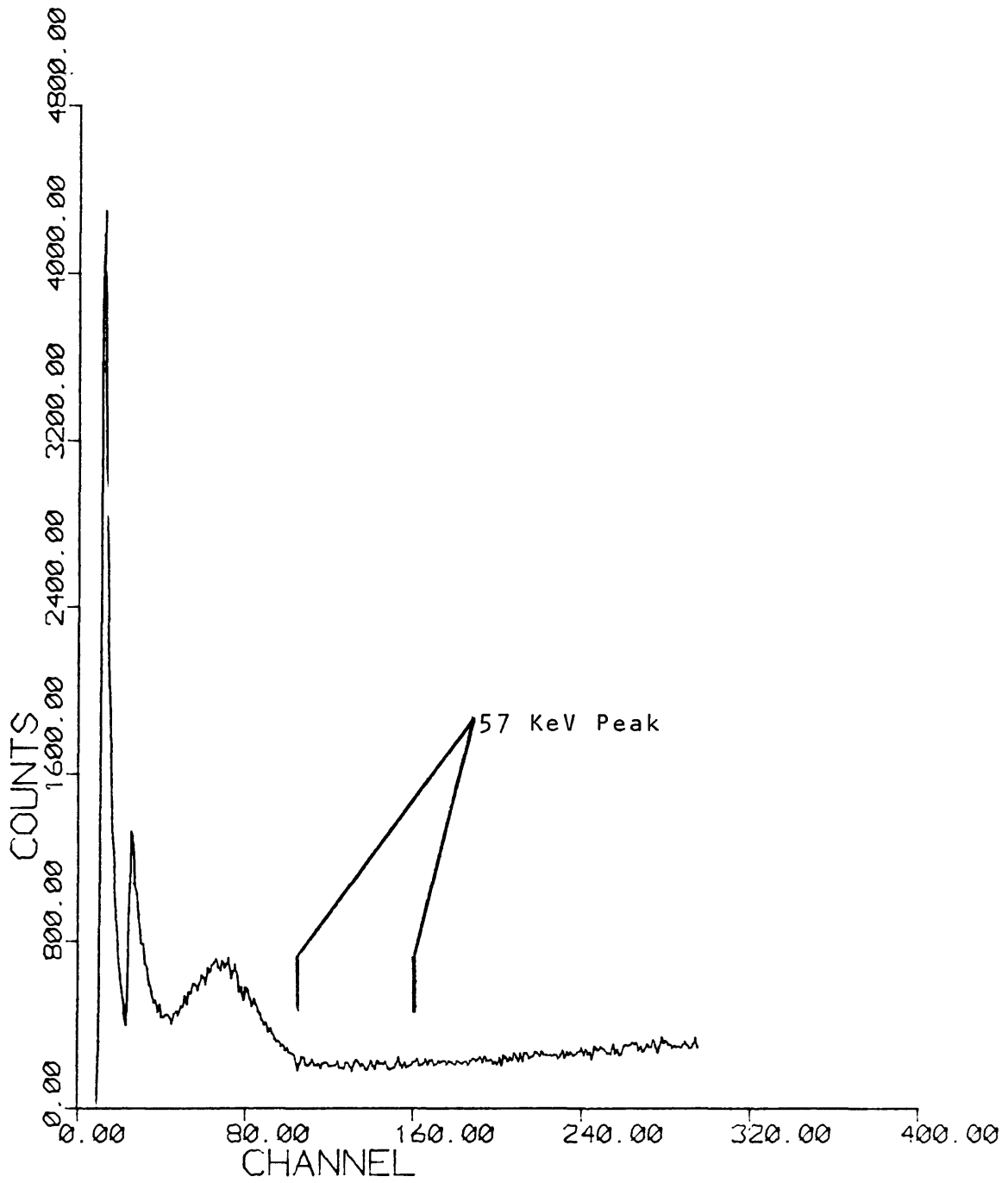


Figure 12: Energy Spectrum of 14.1 MeV Neutron Activation Experiment

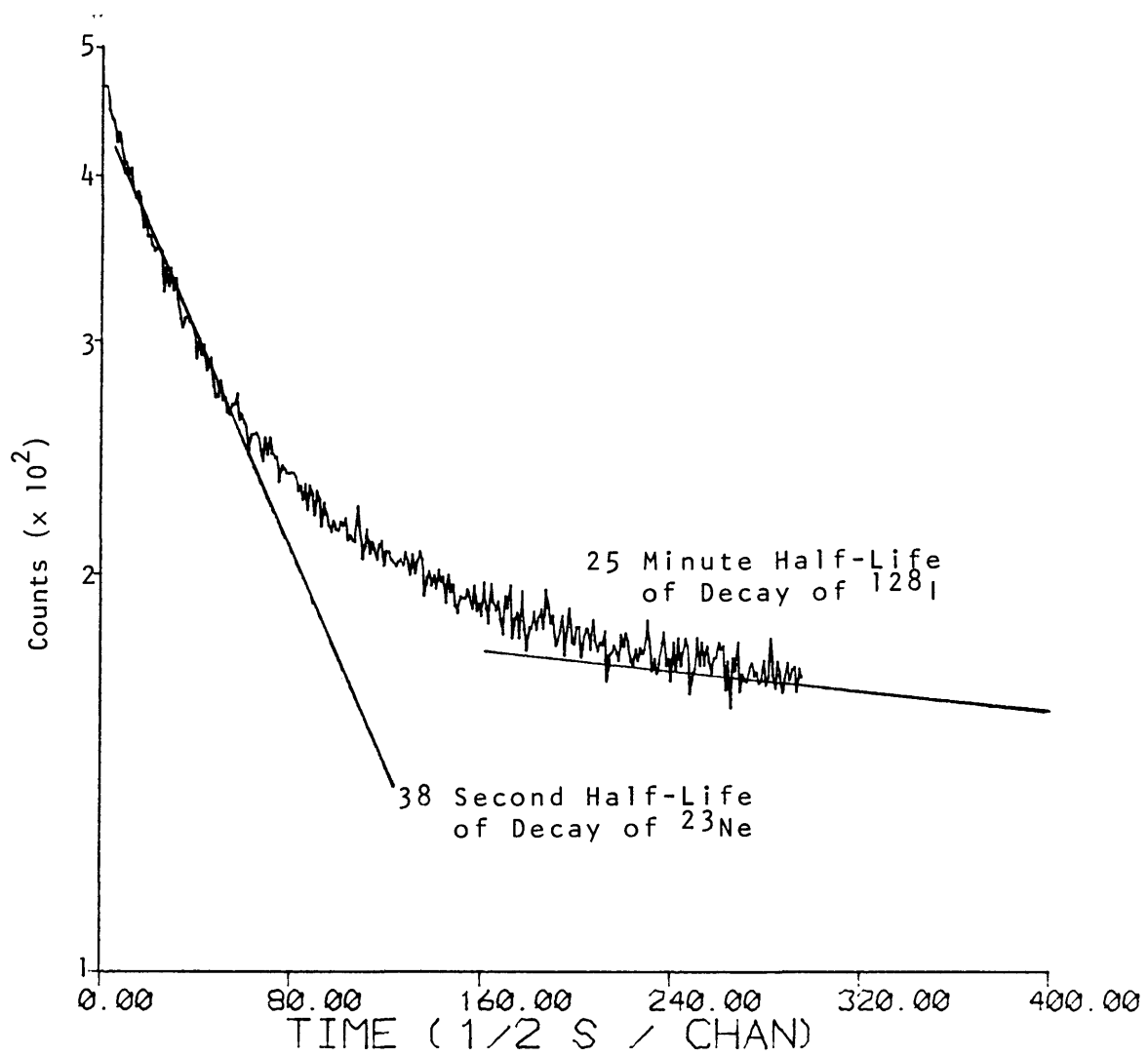


Figure 13: Logarithmic Multiscale Plot of Peak Region Following 14.1 MeV Neutron Activation Experiment

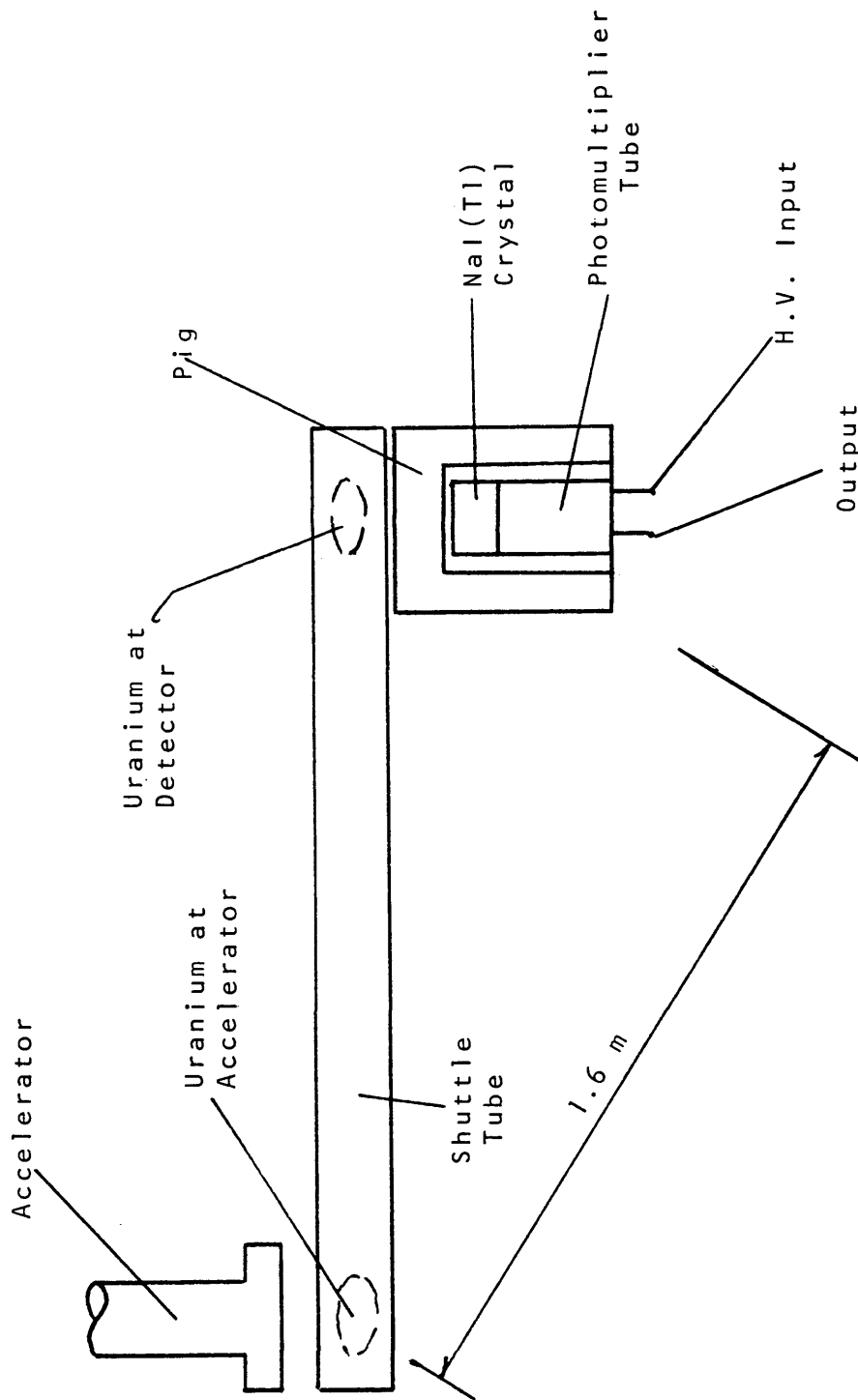


Figure 14: Experimental Setup for 14.1 MeV Bombardment Using Uranium Shuttle

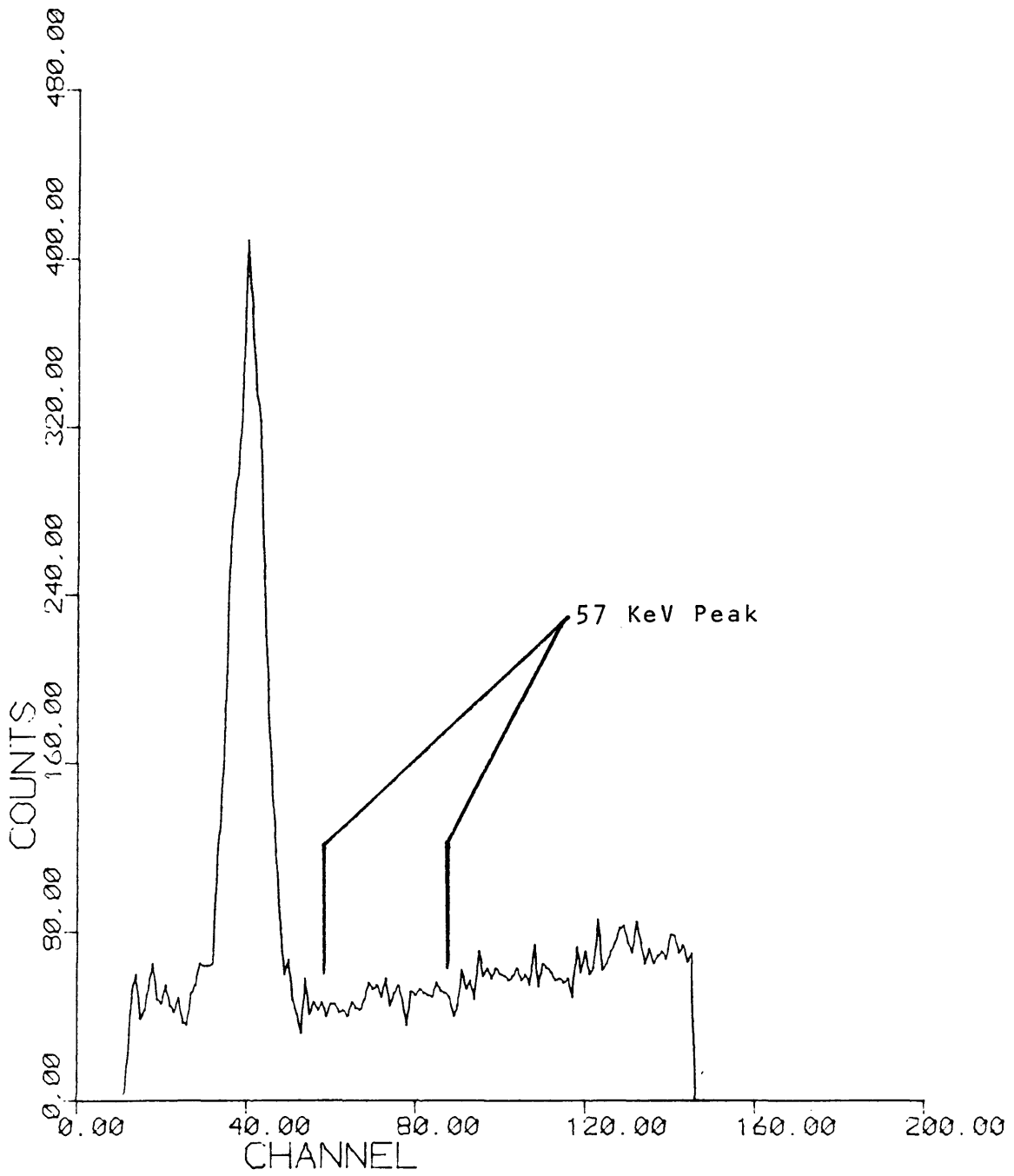


Figure 15: Energy Spectrum of 14.1 MeV Uranium Shuttle Experiment

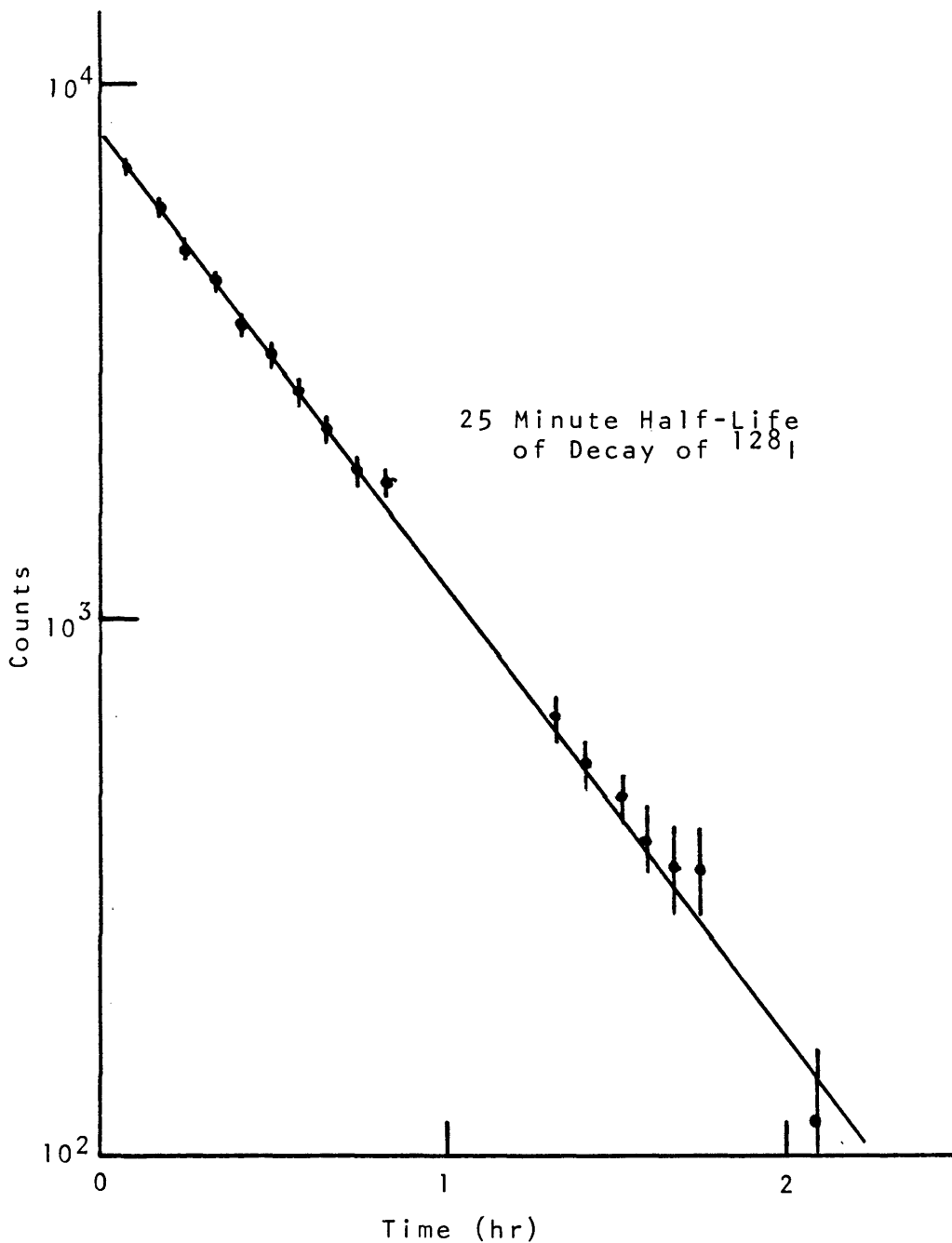


Figure 16: Multiscale of Peak Region Following 14.1 MeV Uranium Shuttle Experiment

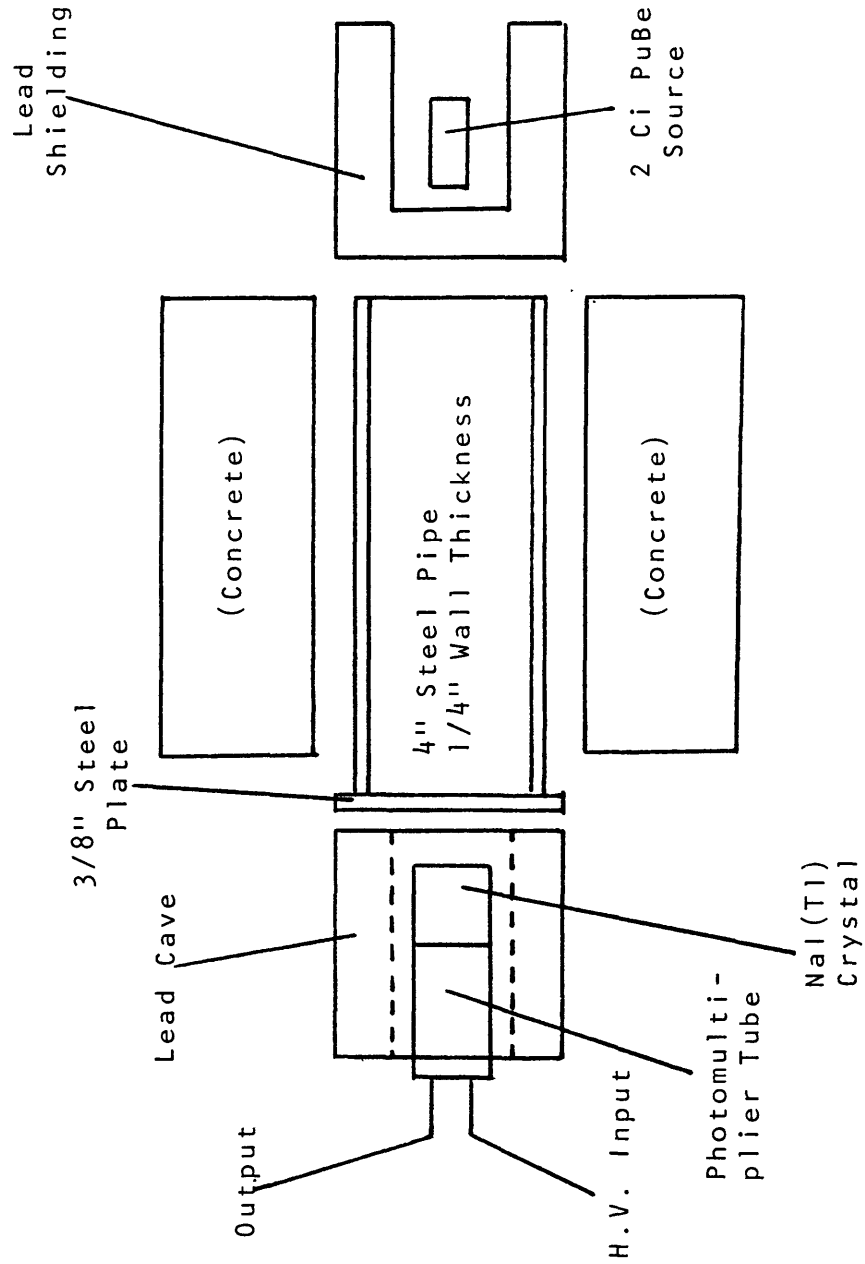


Figure 17: Experimental Setup to Determine Environmental Dependence

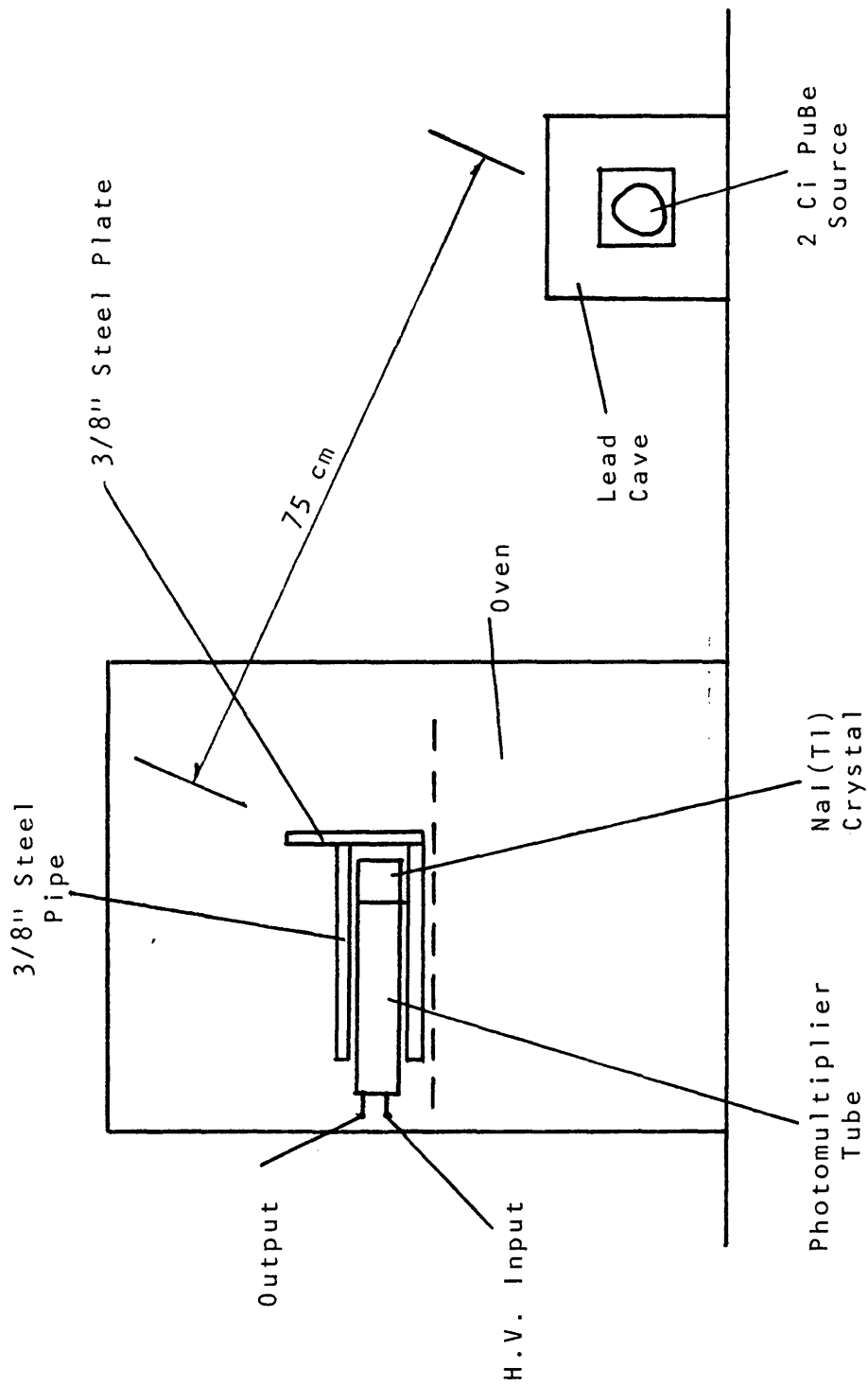
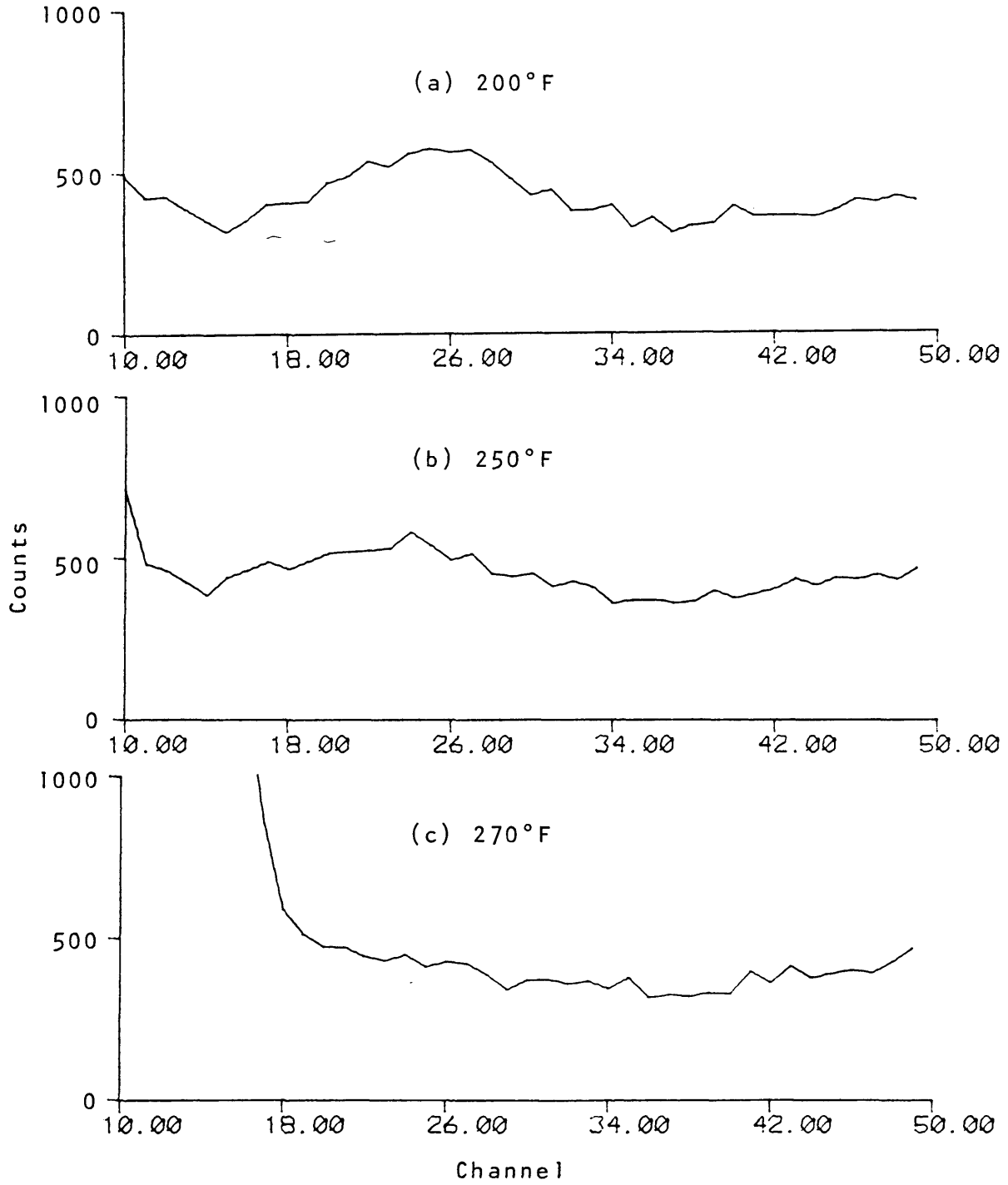


Figure 18: Experimental Setup to Determine Temperature Dependence

Figure 19: Energy Spectrum Illustrating Thermo-electric Encroachment Upon 57 KeV Peak



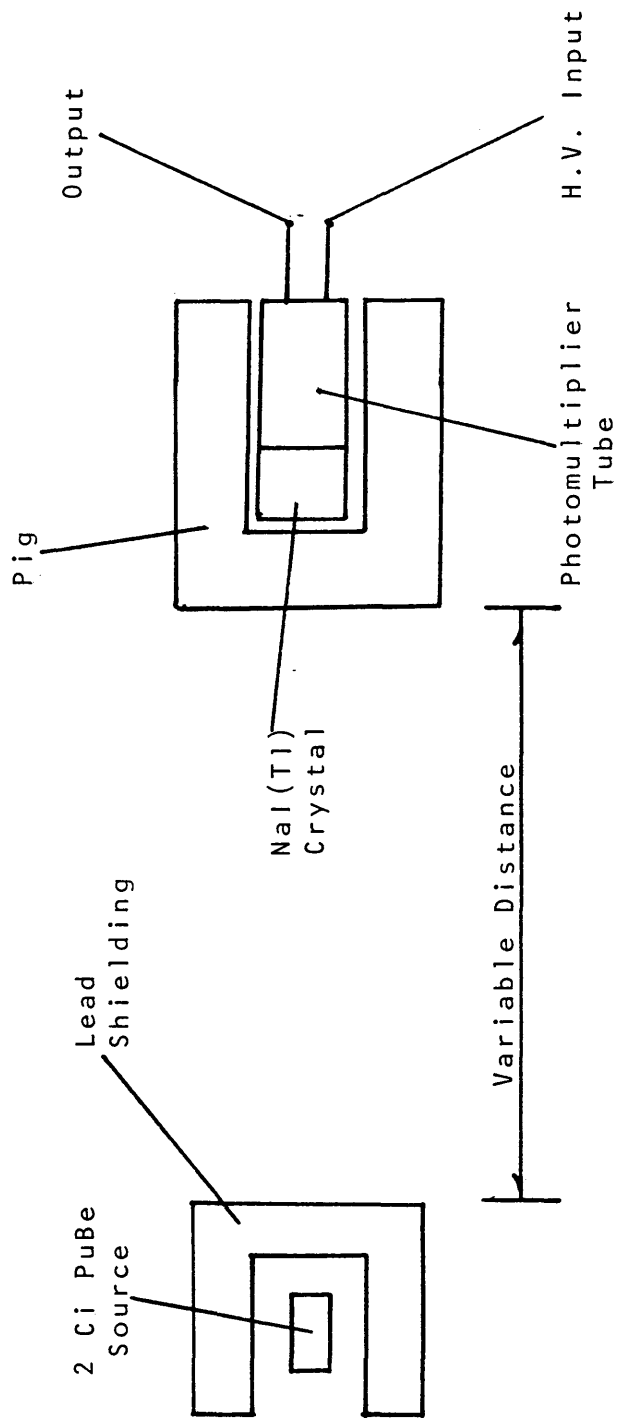


Figure 20: Experimental Setup to Determine Detector Response to High Neutron Flux

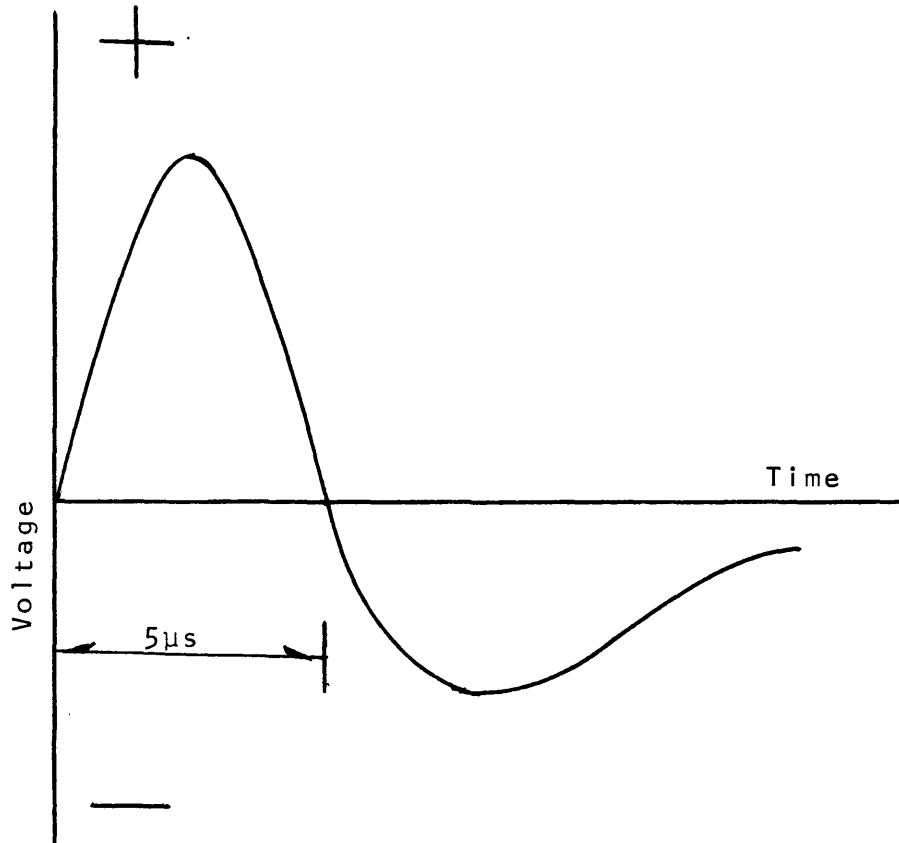


Figure 21: Pulse Shape of Differentially Amplified Photomultiplier Tube Output

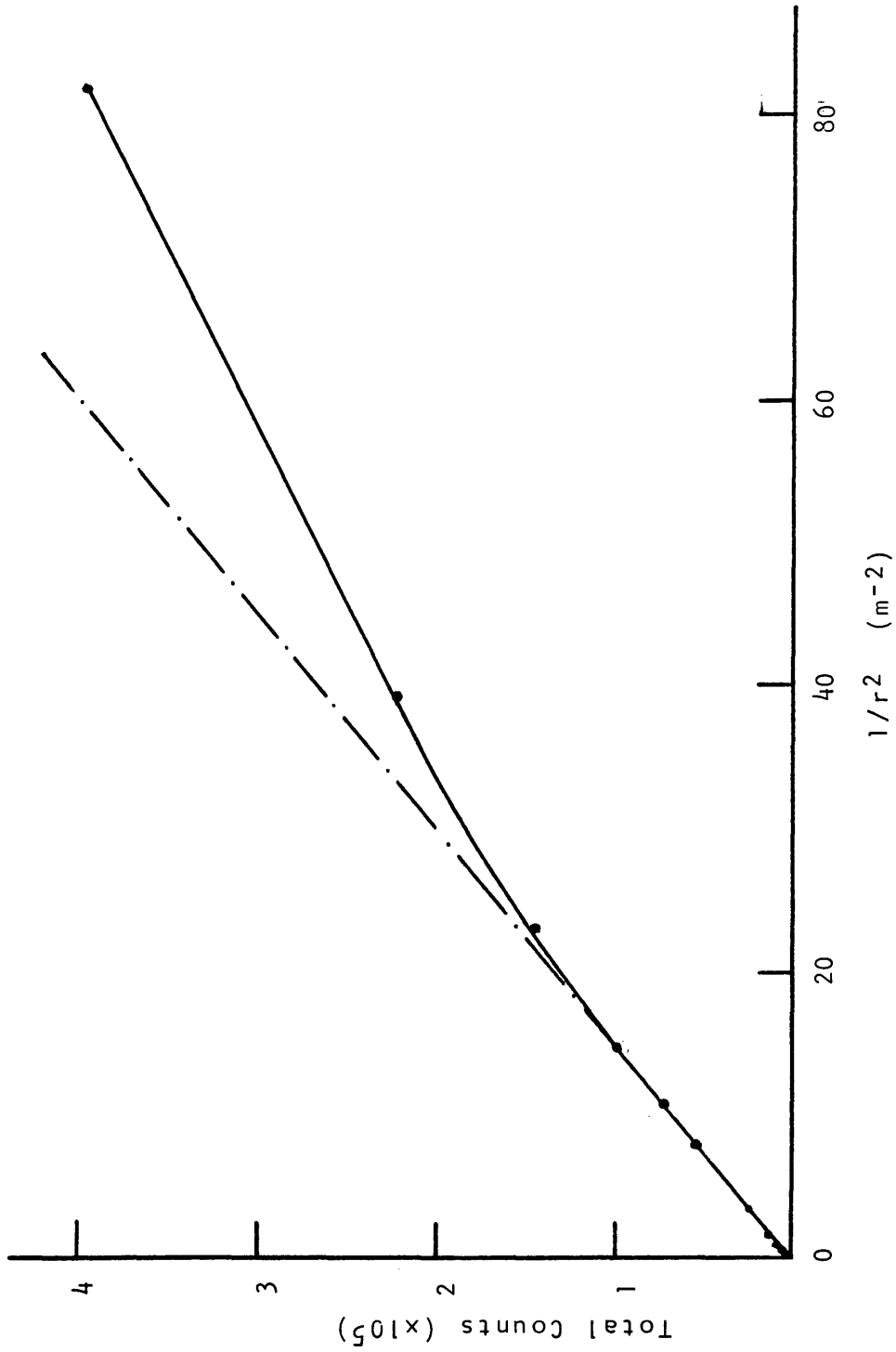


Figure 22: Detector Count Rate vs. $1/r^2$, 5-Minute Samples;
A Plot of Table III.

APPENDIX A

CURVEFITTING PROGRAM

The curvefitting program inputs data from the multichannel analyzer that has been columnized and, after it is given the locations of the channels of interest and the peak, fits the background to either a binomial or an exponential decay of the form $A + Be^{-Cx}$, x being the channel number. It then subtracts the background curve calculated from the raw data, giving the areas of the peak. The peak is fitted to a Gaussian distribution, and the area of the Gaussian is output. Numerous TTY plot options are offered.

To fit the curves, the program compresses the data horizontally into integer bins to make a total of less than 60 channels and uses least-squares fitting on the compressed data. A list of the compressed data can be obtained.

EX MASTER,FLIP
 [22:21:46]
 FORTRAN: MASTER
 MAIN.
 FORTRAN: FLIP
 FLIP
 LINK: LOADING
 [LNKXCT MASTER EXECUTION]

IF YOU HAVE A FILE, TYPE 19.6:
 19.6

TYPE THE 5-CHAR. FILENAME.
 PBCAL

GIVE ME THE FIRST AND LAST CHANNEL NUMBERS:
 80,260

HOW MANY INCHES LONG DO YOU WANT THE DATA?
 (NO GREATER THAN 10 INCHES-- 1 IN.= 6 DATA PTS.)
 4

EACH BIN CONTAINS 7 CHANNELS.
 IF YOU WISH MERELY A PLOT, TYPE 19.6

WHAT ARE THE PEAK-WIDTH CHANNELS?
 140,240

SCALED: 8,23

QUADRATIC=1,EXPONENTIAL=2.
 2

BACKGROUND EQUATION: $1156.0060000 + 1174.6710000 * \exp(-CHAN * 0.3041982)$
 PEAK TOTAL IS $0.6501052E+04 + OR - 0.1593330E+03$

DO YOU WANT A PLOT? (19.6)

HORIZONTALLY COMPRESSED PEAK SOLVES THIS GAUSSIAN:
 SIGMA= 3.0528340 MEAN= 16.7628800 AMP.= 0.9890823E+03
 AREA = 0.7568775E+04
 NEW FILE=1,PLOT=2,EXIT=3.
 2

LINEAR=1; SQUARE ROOT=2; NATURAL LOG=3.

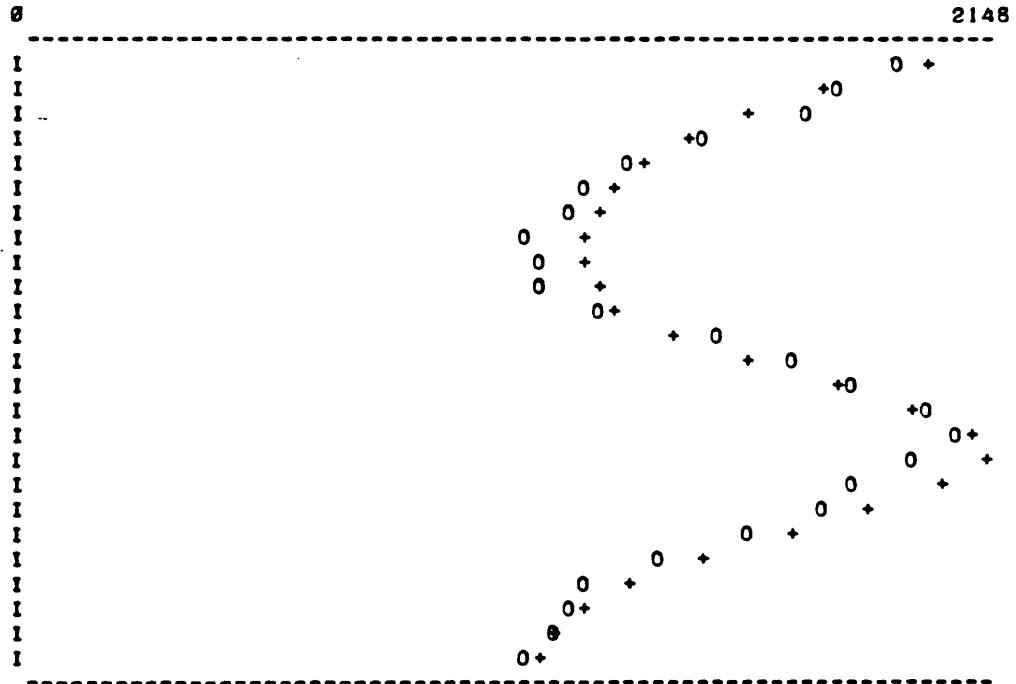
1

WHAT SYMBOL DO YOU WANT FOR THEORETICAL DATA?

+

AND FOR TRUE DATA?

0



IF YOU WANT TO COMPUTE SOME MORE, TYPE 19.6.

NEW FILE=1,COMPRESSED LIST=2,NEW PLOT=3,BYE=4

4

STOP

END OF EXECUTION

CPU TIME: 4.53 ELAPSED TIME: 8:15.78

EXIT

.

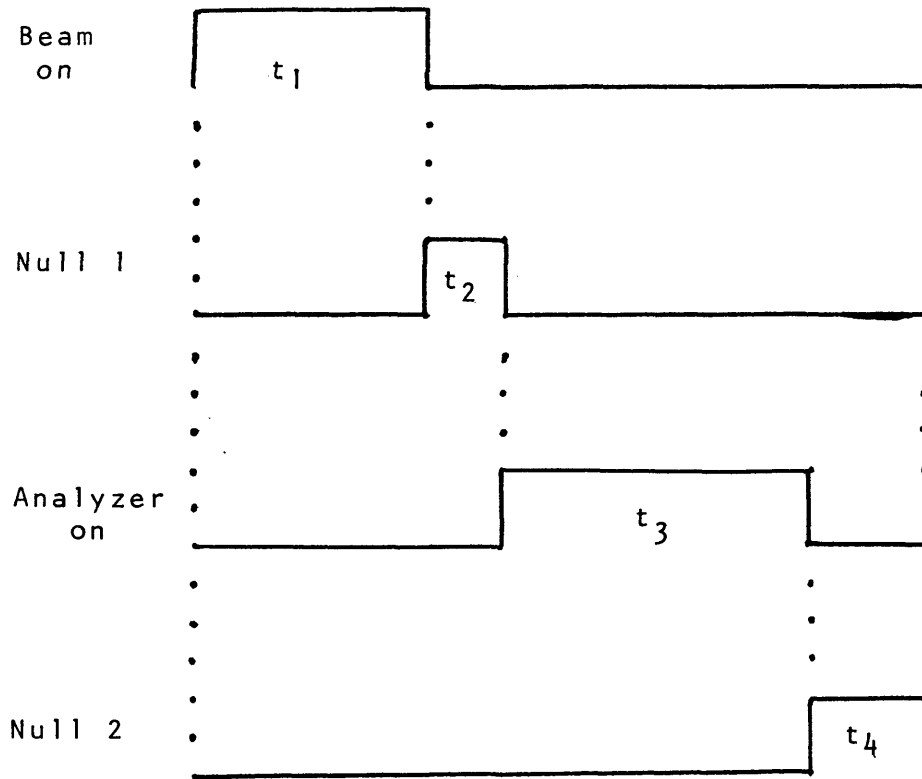
APPENDIX B

SEQUENCING BOX

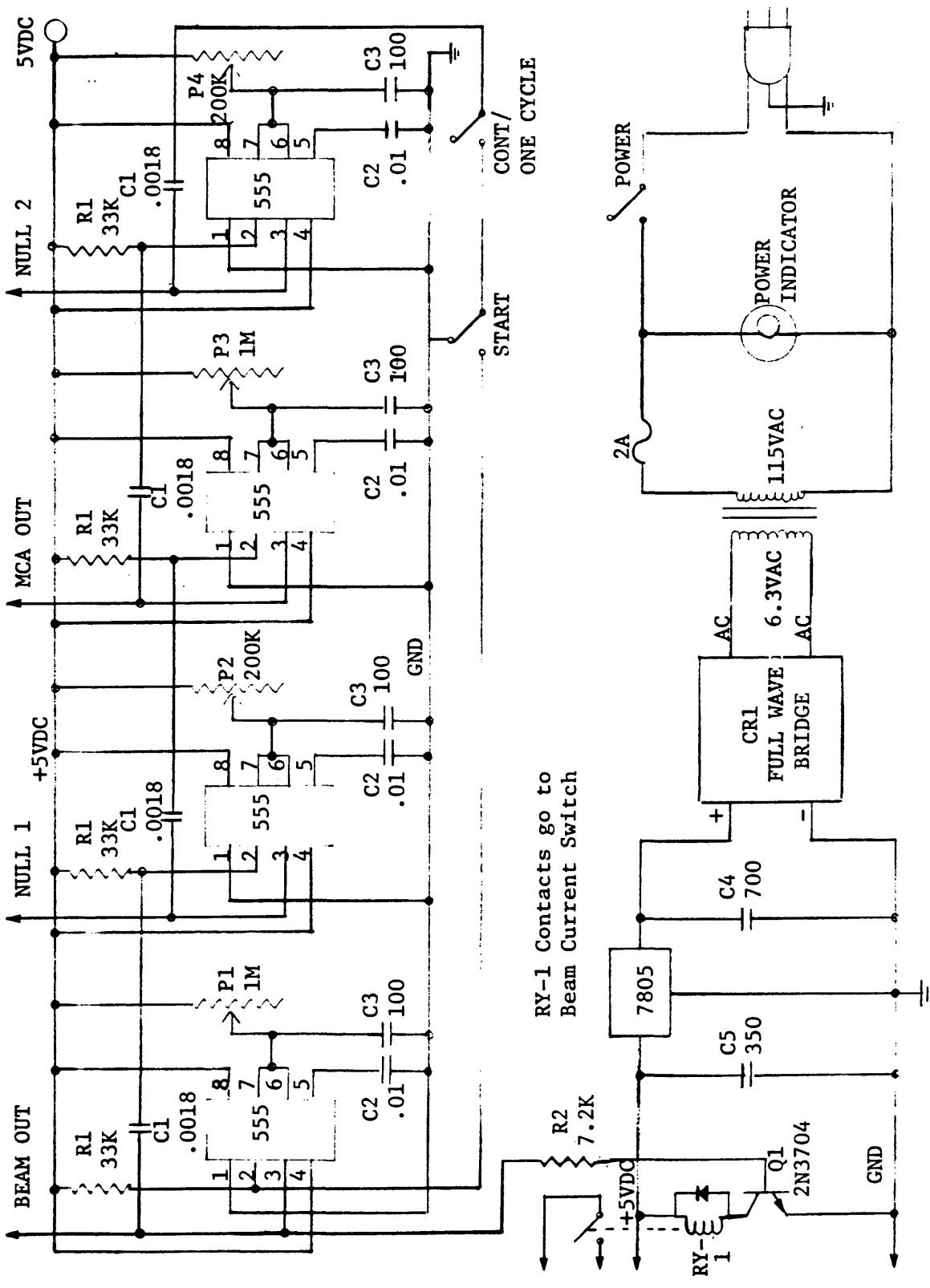
The sequencing box is designed to automatically turn the accelerator beam on and off, wait, turn the multichannel analyzer on and off, wait, and repeat the cycle if desired. Each time interval can be preset by the trimpots on the face of the box (P1-P4). The beam is turned on and off by closing and opening a solenoid switch in the beam current circuit, while the MCA is operated by sending a 4 volt gate signal.

The sequencing is actuated by a momentary switch, and one-cycle/continuous operation is selected by a simple toggle switch. Throwing the toggle to one-cycle during a sequence terminates it before the neutron beam is triggered on the next cycle.

Triggering Sequence



$t_1 + t_2 + t_3 + t_4 = T,$
the retriggering period.



SEQUENCING BOX SCHEMATIC

APPENDIX C

APPROXIMATION OF EXPECTED DELAYED

FISSION NEUTRONS

Assume the area of the U_3O_8 presented to the flux is 1 square inch. So the fraction of the total produced neutrons through the U_3O_8 (assume 10^8 n/s) can be found by:

$$\phi = [1/4\pi r^2] \times 10^8 \text{ n cm}^{-2} \text{ s}^{-1}.$$

$\sigma = 2 \times 10^{-24} \text{ cm}^2$, for fission of ^{238}U (an overestimate, since a large percentage of the source neutrons will have lost enough energy to be below the Q-value for ^{238}U fission), from Reference 1. By Reference 1, 4% of the fissions produce a delayed fission neutron (again, making the high assumption that predominantly ^{238}U fissions).

$N =$ the amount of Uranium in the sample, which is $[(6 \times 10^{23} \text{ atoms/mole})/280 \text{ g/mole}] \times 20 \text{ g} = 4 \times 10^{22}$ atoms.

The number of reactions produced in a time t_b is $N_p = \phi \sigma N (1 - e^{-\lambda t_b}) / \lambda$, λ being the decay constant of the specie produced (found by integrating the rate on a thin target $dN_p/dt = \phi \sigma N e^{-\lambda t}$). For our example, we must multiply by .04, the probability of producing a delayed fission neutron.

The duration of bombardment, t_b , must be known, as well as t_w , the waiting time between bombardment and detection, and t_c , the sampling interval. A fraction of the number of produced neutrons, $(1 - e^{-\lambda t_w})$, is lost in the waiting process by radioactive decay, allowing only the fraction $e^{-\lambda t_w}$ to be detected. Of those remaining, only the fraction $(1 - e^{-\lambda t_c})$ will pass through the detector, and only a small fraction of those will be detected due to the efficiency of the detector, ϵ .

Because there are many chains with different half-lives and relative abundances f (Reference 1), it is necessary to multiply each separate calculation by its relative abundance and sum all the calculations to yield the total detected DFN's:

$$N_d = .04N\phi\sigma\epsilon n \sum_i f_i/\lambda_i (1 - e^{-\lambda_i t_b}) e^{-\lambda_i t_w} (1 - e^{-\lambda_i t_c}),$$

where n is the number of times the sequence is completed, and $\lambda = \ln(2)/t_{1/2}$.

REFERENCES

1. James J. Duderstadt and Louis J. Hamilton, Nuclear Reactor Analysis, John Wiley & Sons, New York, p. 64, (1976).
2. Ibid., p. 64.
3. Kendrick L. Killian, Measurement of Fast Neutron Detection Efficiency for a NaI(Tl) Scintillator, M.Sc. Thesis, Colorado School of Mines, p. 36, (1978).
4. F. E. Cecil, K. Killian, and M. Rymes, "Evaluation of NaI(Tl) Scintillator as a Fast Neutron Monitor," IEEE Transactions on Nuclear Science, Vol. NS-26, No. 1, p. 1487-1489, (1978).
5. F. E. Cecil, K. Killian, and M. Rymes, To Be Published, Physical Review C, (1979).
6. J. VanLoef and D. A. Lind, "Measurement of Inelastic Scattering Cross Sections for Fast Neutrons," Physical Review, 101, p. 103-113, (1956).
7. Kendrick L. Killian, op. cit., p. 29.
8. Peter J. Eisler and Paul Huppert, "A Nuclear Geophysical Borehole Logging System," Nuclear Instruments and Methods, 158, p. 579-586, (1979).
9. M. R. Wormald, C. G. Clayton, "Some Factors Affecting Accuracy in the Direct Determination of Uranium Delayed Neutron Borehole Logging," Exploration for Uranium Ore Deposits, Vienna, International Atomic Energy Agency, p. 427-469, (1976).
10. W. W. Givens, W. R. Mills, C. L. Denvis, and R. L. Caldwell, "Uranium Assay Logging Using a Pulsed 14 MeV Neutron Source and Detection of Delayed Fission Neutrons," Geophysics, 41, p. 476, (1976).

11. Richard Cecil Smith, "Measured Characteristics of Pulsed Neutron Assaying of Uranium Ore Deposits," IEEE Transactions on Nuclear Science, Vol. NS-26, No. 1, p. 1579-1583, (1978).
12. William S. Lyon, Guide to Activation Analysis, Princeton, New Jersey, D. Van Nostrand Company, p. 46, (1964).
13. Ibid., p. 34.
14. William S. Lyon, op. cit., p. 34.
15. D. I. Garber and R. R. Kinsey, Neutron Cross Sections, Vol. 2, Edition 3, National Neutron Cross Section Center, Brookhaven National Laboratory, Upton, New York, p. 53, (1976).
16. J. Duray, Private Correspondence, 1979.
17. H. Landsberg, "Note on the Frequency Distribution of Geothermal Gradients," American Geophysical Union Transactions, 27, p. 549-551, (1946).